Fibrous wearable and implantable bioelectronics

Behnam Sadri,[1] Wei Gao[1,*]

[1]Andrew and Peggy Cherng Department of Medical Engineering, Division of Engineering and Applied Science, California Institute of Technology; Pasadena, California, 91125, USA.

*Email: weigao@caltech.edu

Abstract

Fibrous wearable and implantable devices have emerged as a promising technology, offering a range of new solutions for minimally invasive monitoring of human health. Compared to traditional biomedical devices, fibers offer a possibility for a modular design compatible with large-scale manufacturing and a plethora of advantages including mechanical compliance, breathability, and biocompatibility. The new generation of fibrous biomedical devices can revolutionize easy-to-use and accessible health monitoring systems by serving as building blocks for most common wearables such as fabrics and clothes. Despite significant progress in the fabrication, materials, and application of fibrous biomedical devices, there is still a notable absence of a comprehensive and systematic review on the subject. This review paper provides an overview of recent advancements in the development of fibrous wearable and implantable electronics. We categorized these advancements into three main areas: manufacturing processes, platforms, and applications, outlining their respective merits and limitations. The paper concludes by discussing the outlook and challenges that lie ahead for fiber bioelectronics, providing a holistic view of its current stage of development.

1. Introduction

The rapid advancements in wearable and implantable electronics have revolutionized the field of medicine, offering a new era of continuous monitoring and personalized therapy for a wide range of health conditions. These emerging flexible electronic platforms can seamlessly integrate to biological tissues,[1,2] enabling real-time data collection, transfer, and improving monitoring of disease progression and diagnostics.[3,4] However, wearable and implantable electronics often suffer from limited energy resources,[5] costly fabrication,[6] non-scalable manufacturing, and foreign body

reaction[7] primarily due to mechanical mismatch with surrounding tissues.[8] On the other hand, bioelectronics on elastomeric substrates, including polyimide, PDMS, and silk, have demonstrated remarkable biocompatibility, sensitivity, and flexibility. However, their bulky and non-porous nature restricts gas permeation to surrounding tissues, leading to potential adverse effects due to their inherent mechanical mismatch and limiting their long-term use by promoting microphage formation. To overcome these challenges, the next generation of wearable and implantable bioelectronics requires delivering high performance with minimally invasive, mechanically compliant, and sterilizable platforms.

Fibers are one of the exciting platforms to host bioelectronics with promising strong, easy-to-handle, and deformable properties.[9] They are ubiquitous in both woven and non-woven forms, having been an integral part of human life for thousands of years and appearing in a wide range of everyday products, from clothing[10] to wound dressings.[11] The invention of optical fibers by Colladen and Bobinet in the early 1800s marked a turning point in the utilization of fibrous device technologies,[12] leading to the exploration of new applications beyond the transmission of information over long distances.[13] One of these exciting adventures is integrating fibrous structures with wearable and implantable bioelectronics.[14] Significant advances have been made recently towards the fabrication of functional fibrous sensors and actuators, by merging the scalable and cost-effective production of fibers with functional electronics.[15] These innovations have a broad range of applications, ranging from the development of wearable batteries[16,17] to the monitoring of neuron activity.[18] While there has been significant progress in fabricating functional fibrous wearables and implants, a comprehensive and systematic review of the latest advancements in fabrication methods, platforms, and applications of fiber bioelectronics is crucial for advancing the field. Despite several comprehensive reviews available on the general topic of functional fibers and their applications,[8,15,19–22] a review that specifically outlines the key advances in fabrication, materials, and applications of fibrous wearable and implantable platforms is currently lacking.

This review provides an overview of recent advances in fibrous bioelectronics and their applications (Figure 1). Here, we have divided the advancements in this field into three main categories: (i) fabrication methods, (ii) platforms, and (iii) applications. We first review spinning methods, additive manufacturing techniques, and emerging platforms to controllably manufacture fibrous bioelectronics. We then summarize the major developments in fibrous materials used in electronic platforms and their fibrous interface with biological tissues. Finally, we delve into the

application of these fibers as power resource platforms, thermal management interfaces, wearable devices, and implantable bioelectronics. Given there are excellent reviews available on the manufacturing of optical fibers and their applications,[23–28] we have chosen not to discuss them in this review. However, we will highlight their recent and exceptional advancements in integrating with electronics for biomedical applications related to in-vivo stimulation and recording.

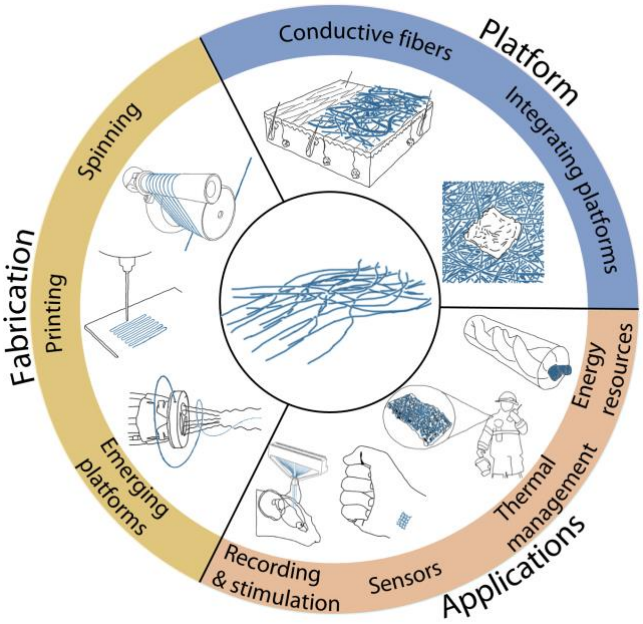

Figure 1. An overview for fibrous wearable and implantable bioelectronics, discussed within three main categories: fabrication, platforms, and applications. Main discussions on the fabrication section cover spinning, printing, and emerging platforms. These platforms are further categorized into two main types: conductive fibers and integrating platforms. Additionally, the main topics of discussion for applications include recording and stimulation, sensors, thermal management, and energy resources.

2. Fabrication Methods

The development of wearable and implantable devices requires the creation of fiber-based devices that can effectively deliver electrical signals and display various functionalities. Fabrication methods play a critical role in determining the performance and functionality of these fibers. In this section, we will review the current state of the art, advantages, and challenges in using spinning methods, additive manufacturing, and emerging manufacturing methods, as board categories for fabrication techniques of the fibrous wearable and implantable electronics. The authors acknowledge that certain fiber fabrication techniques, such as molding,[29] may not be readily

categorized into the methods discussed in this paper. Nonetheless, this section includes a discussion on the principles of analogous techniques, such as templating, with the aim of providing a holistic view of the current landscape of fiber manufacturing methods.

2.1 Spinning methods

To meet the demands of improving the performance of fibrous bioelectronics, there is a growing need to reduce the diameter of the fibers, as this can increase the active surface area and improve performance without the need for a larger device package. Electrospinning is one of the established methods to produce nanofibers by applying an electric field at the tip of the nozzle, enhancing the tangential forces to create tiny jets and produce nanofibers, which are collected on a grounded electrode (Figure 2a).[30–32] This method of fabrication has gained significant attention as a facile, low-cost technique, and versatile platform for producing nanofibers from a diverse range of dielectric materials.[33,34] Its inventor, John B. Fenn, was even awarded the Nobel Prize in Chemistry in 2002, highlighting its importance and potential impact in the scientific community.[35] Over the years, electrospinning has evolved into a method to provide nanofibrous platforms, compatible with selective chemical or physical deposition techniques (Figure 2b).[36] Moreover, electrospinning is one the few methods that can perform controlled deposition of nanofibers, by often manipulating surface charge of the grounded electrode or rotating it (Figure 2c).[37] While electrospinning is an accessible, simple, and one-step manufacturing technique, it is limited in working with spinning solutions of high surface tension, low viscosity, or high electrical conductivity. Therefore, the range of fiber properties produced by this method is limited.[38]

Thermally drawn spinning is another exciting method for scalable fabrication of fibers with uniform quality (Figure 2d).[39–52] This fabrication method is compatible with a wide range of polymeric materials ranging from thermoset to thermoplastics.[21] Thermally drawn spinning can produce multi-material fibers with high precision (Figure 2e),[40] imparting unique mechanical properties and enabling their use for exciting applications such as artificial muscle (Figure 2f).[39] This method, however, requires a complex process with high energy consumption owing to often high processing temperature, leading to elevated production cost for the fibers.

The other common method to produce polymeric fibers is through extruding polymeric solution from a spinneret inside a coagulation bath, often called wet spinning (Figure 2g).[53–62] This method

can produce fibers from thermally sensitive polymers, capable of controllably generating fine structures within the fiber (Figure 2h & i).[53,55] Moreover, controlling processing conditions in wet spinning can lead to a high degree of orientation in fiber, thus strengthening the fiber structure. While wet spinning has become increasingly popular due to its ability to offer precise control over fiber morphology, its utilization as an industrial-scale manufacturing process is limited due to the process being diffusion-limited and the presence of solvent residuals.

A spinning method to continuously produce fibers in large-scale is solution blow spinning (Figure 2j).[63–67] In this method, air flow is responsible to provide the necessary shear stress to produce nanofibers from polymer solutions fed into spinneret. This facile method is capable of large-scale production of nanofibers and compatible with a wide range of materials including metals (Figure 2k).[68] Despite its simple, one step fabrication mechanism, poor fiber morphology and random deposition of fibers are some of the major disadvantages for this process (Figure 2l).[69]

Fiber production through spinning methods, including wet and dry spinning, are known to exhibit inconsistencies throughout the fiber due to the diffusion-limited mechanisms involved, which are highly sensitive to environmental factors such as temperature and polymer concentrations. Similarly, while electrospinning presents a simple manufacturing method, producing consistent fibers is exceedingly challenging as the charge concentration at the nozzle tip is highly dependent on small variations in polymer conductivity and viscosity. Another conventional fiber spinning method, air spinning, can generate fibers on a large scale but lacks the ability to produce fibers with higher aspect ratios, with limited control over fiber formation from air forces in the spinnerets. In contrast, the melt spinning technique offers a reliable means of producing fibers on a large scale, though its production rate still lags conventional industrial standards.

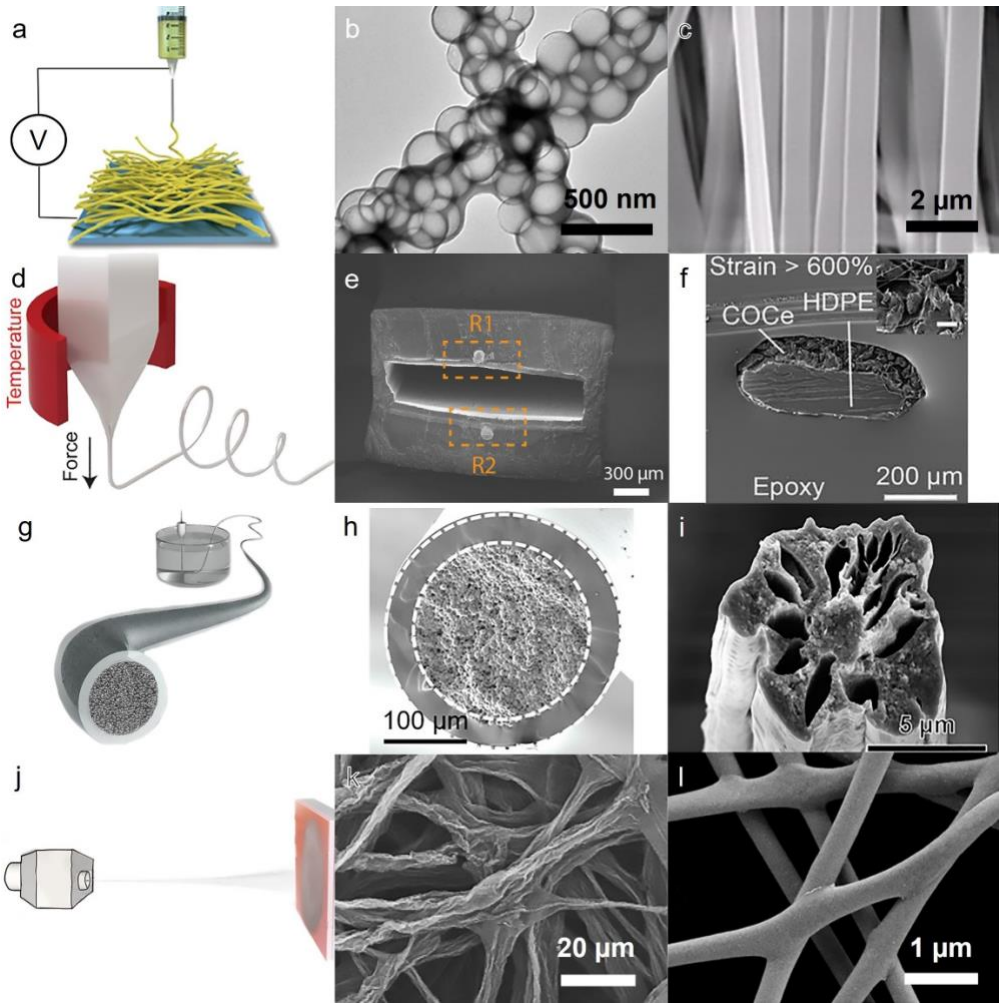

Figure 2. Fabrication of fibers through spinning methods. (a) Schematics of electrospinning setup. Reproduced with permission from Wang et al., Adv. Mater. 34, e2108325 (2022). Copyright 2022 John Wiley and Sons.[70] (b) Chemical deposition of Ag Nanoparticles on the surface of electrospun nanoparticles. Reproduced with permission from Fang et al., Sci. Adv. 7, eabg3626 (2021). Copyright 2021 American Association for the Advancement of Science.[36] (c) Scanning electron microscopy (SEM) image of aligned smooth surface of produced electrospun collagen/silk composite fibers. Reproduced with permission from Xu et al., Sci. Adv. 6, eabc2036 (2020). Copyright 2020 American Association for the Advancement of Science.[37] (d) Schematic illustration for melt spinning techniques. Reproduced with permission from Kanik et al., Science 365, 145 (2019). Copyright 2019 American Association for the Advancement of Science.[39] (e) Complex architecture of thermally drawn fiber made from SBS, liquid metal, and conductive composite. Reproduced with permission from Dong et al., Sci. Adv. 8, eabo0869 (2022); licensed

under a Creative Commons Attribution (CC BY) license.[40] (f) Excellent fiber morphology displayed in cross-sectional SEM image of the thermally drawn fibers. Reproduced with permission from Kanik et al., Science 365, 145 (2019). Copyright 2019 American Association for the Advancement of Science.[39] (g) Schematic illustration of wet spinning process outlining its key components. (h) Cross-section of a core/shell microfibers made from composite liquid metal/PVDF-HFP-TFE core with PEGDA shell. G-h, reproduced with permission from Zheng et al., Sci. Adv. 7, eabg4041 (2021). Copyright 2021 American Association for the Advancement of Science.[53] (i) Cross section of a porous polyacrylonitrile/carbon fiber made from wet spinning. Reproduced with permission from Gao et al., Sci. Adv. 6, eaaz4191 (2020). Copyright 2020 American Association for the Advancement of Science.[55] (j) Schematics of solution blow spinning setup. Reproduced with permission from Lin et al., Npj Flex. 6, 1 (2022); licensed under a Creative Commons Attribution (CC BY) license.[63] (k) Non-woven graphene fiber realized by blow spinning solution. Reproduced with permission from Liu et al., Nano Lett. 21, 5116 (2021). Copyright 2022 American Chemical Society.[68] (l) Blown-spun silver (Ag) nanofibers and their connected junctions. Reproduced with permission from Lin et al., Npj Flex. 3, 1 (2019). Sci Adv 8, eabo0869 (2022); licensed under a Creative Commons Attribution (CC BY) license.[69]

2.2 Additive manufacturing

The advancements in additive manufacturing have enabled the creation of high-performance fibers with unique geometries and improved mechanical properties. Additive manufacturing techniques are generally based on lithography, sintering, or extrusion-based systems.[71] Fiber fabrication through additive manufacturing is primarily based on extrusion forces, offering exceptional electrical and mechanical properties.[72] In this process, the ink solution is often heated and extruded through a nozzle[73] (Figure 3a) to produce sub-millimeter resolution fibers with precise deposition (Figure 3b & c),[74,75] which opens up new functionalities for fibrous platforms. However, one of the major challenges of this method is achieving a high-resolution print from a wide range of polymeric inks.

To solve this problem, electrohydrodynamic (EHD) printing exploits electric fields to produce nanofibers with the help of tangential electrical forces exerted at the tip of the nozzle (Figure 3d).[76–80] Despite being invented recently,[81] this fabrication method is currently capable of controllable deposition of nanofibers (Figure 3e)[77] and layer by layer printing (Figure 3f).[78] The production of

fibers through EHD printing, however, faces major challenges on the scalability and device integration. Recently, Inflight printing, as an emerging form of draw spinning, offered to solve these problems using a one-step printing technique, printing 1- to 3-**μ**m fiber through a core/shell nozzle with a viscous sheath and a conductive core (Figures 3g & h).[82] This method is capable of printing suspended fibers, imparting sensory function to 3D printed fibrous devices. Draw spinning enabled production of flexible metallic fibrous nanomeshes realized by homo cross-junctions and hetero cross-junctions (Figure 3i).[83] While nozzle-based additive manufacturing have predominantly used as a fiber production method, small sized flow chambers, often known as microfluidic channels, are also used to produce fibers (Figure 3j), offering several advantages such as improved fiber uniformity and enhanced control over fiber production with miniaturized setup for fiber production. (Figure 3k & l).[84]

Additive manufacturing techniques are becoming increasingly attractive for large-scale industrial fiber production due to their ability to exert more control over fiber formation and produce consistent properties throughout the fiber. Among these techniques, extrusion-based processes stand out as a prominent example capable of precise fiber deposition and the creation of complex structures on a large scale. Unfortunately, other established additive manufacturing techniques are still in their nascent stage, and the fabrication process remains challenging to control. For instance, electric field in inflight printing or diffusion processes in flow-focusing printing can be difficult to manage, thereby limiting the fiber's consistency, production rate, and overall impact on the fiber production industry.

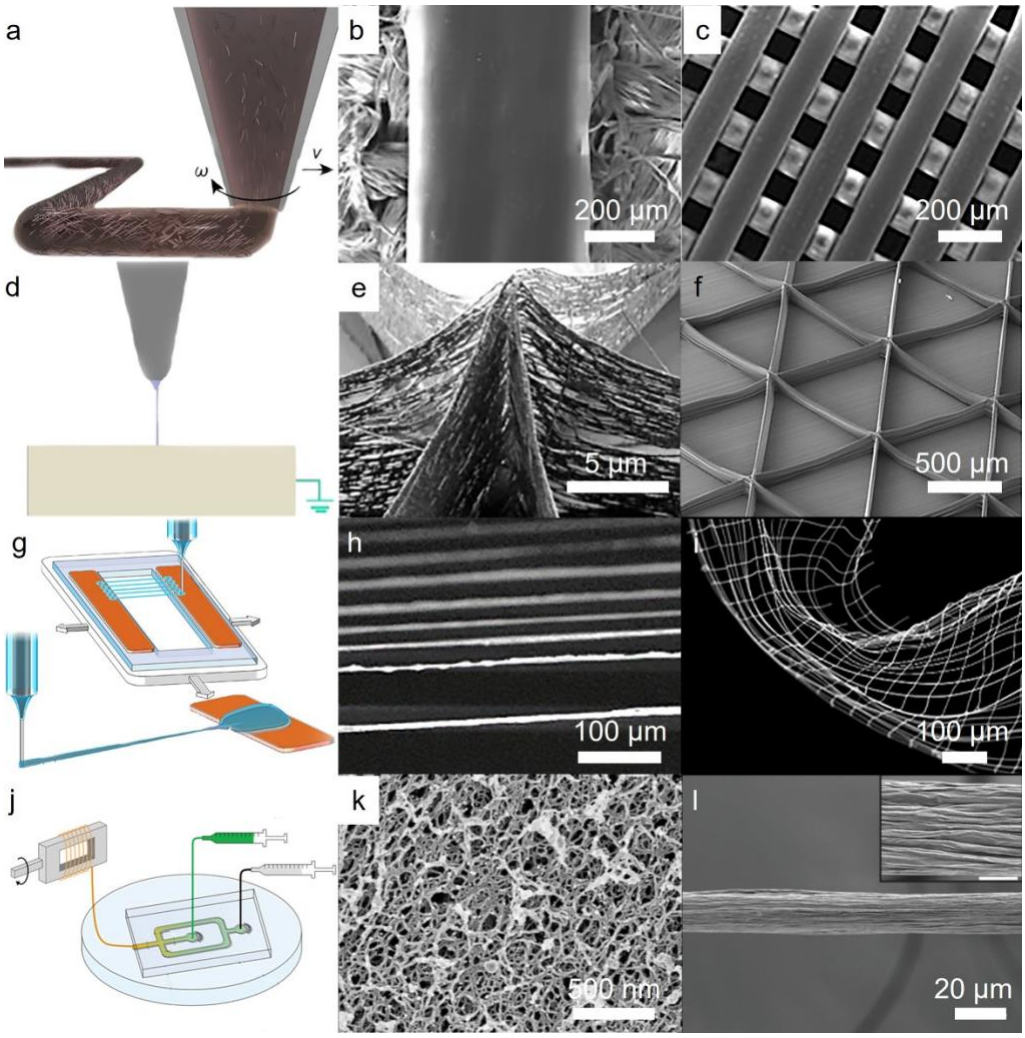

Figure 3. Additive manufacturing techniques to produce fibers. (a) A visual representation of printing fibers using a rotating nozzle to create a helical pattern. Reproduced with Permission from Ref. 73. (b) Structure of fibers manufactured through direct printing, made of CNT core and silk fibroin sheath. Reproduced with permission from Zhang et al., Matter 1, 168 (2019). Copyright 2019 Elsevier.[74] (c) Cartilage Scaffolds realized by extrusion printing. Reproduced with permission from Sun et al., Sci. Adv. 6, eaay1422 (2020); licensed under a Creative Commons Attribution (CC BY) license.[75] (d) Schematics of direct writing EHD printing setup. Reproduced with permission from Kong et al., Nat. Commun. 11, 1 (2020); licensed under a Creative Commons Attribution (CC BY) license.[76] (e) Crossing of three fibrous walls printed by EHD printing, made from polyethylene oxide ink mixed with Ag nanoparticles. Reproduced with permission from Liashenko et al., Nat. Commun. 11, 753 (2020); licensed under a Creative Commons Attribution (CC BY) license.[77] (f) Layer by layer assembly of microfiber realized by EHD printing. These 10

μm size fibers are made from Poly Lactic-co-Glycolic Acid (PLGA). Reproduced with permission from Moon et al., Sci. Adv. 7, eabf5289 (2021). Copyright 2021 American Association for the Advancement of Science.[78] (g) Inflight printing of silver and PEDOT:PSS fibers. (h) Suspended, aligned arrays of Silver/PEDOT:PSS fibers realized by inflight printing. (i) SEM image of curved nanofiber mesh produced by inflight printing. G-I, reproduced with permission from Wang et al., Sci. Adv. 6, eaba0931 (2020); licensed under a Creative Commons Attribution (CC BY) license.[82] (j) Schematic illustration of flow-focusing, microfluidic setup. (k) Dried spun fibers made from protein nanofibrils mixed with polysaccharide and alginate coflowing with polyethylene glycol are realized by microfluidic fiber printing. (l) SEM image of the microfluidic-printed fiber with tightly packed bundles on its surface. J-I, reproduced with permission from Kamada et al., Small 16, e1904190 (2020). Copyright 2020 John Wiley and Sons.[84]

2.3 Emerging manufacturing methods

Emerging fiber manufacturing processes are mainly hybrid methods, combining the advantages of traditionally available fabrication techniques. These emerging platforms are needed for further controlling of fiber deposition, larger scale of fabrication, and compatibility with new generations of materials. To enhance the control on fiber deposition, manufacturing setup comprised of new nozzles with a rotating nozzle capable of air blowing is recently developed to direct the fibers produced along the airstream, mimicking biological tissues that are typically made by aligned collagen fibers by forming similar structures and displaying more uniform deformations (Figure 4a).[85,86] The scalability of fiber production is also extremely important to meet the growing demands and reduce the final cost for production. Using air blowing on a network of nylon threads coated with a variety of viscous spinning solutions, fibers are formed as a result of shear stresses induced by the surrounding air stream (Figure 4b).[87] This method offers nanometer size fibers in larger scale of production while it is compatible with a wide range of materials. Small-sized fibers with high aspect ratio can also be made by using molten polymerous spinning solution. In this method, premade high aspect ratio electrodes are immersed inside the molten polymer solution, allowing self-assembly of polymer fibers on top of an array of microelectrodes and realizing thin, high aspect ratio filaments (Figure 4c).[88] Although most human-made fiber fabrication technologies offer increasing control on fiber morphologies, they still need trained personnel due to their often complicated processes. Inspired by silkworm fiber spinning, microadhesion guided

fiber formation is a simple process, capable of instant/on demand nanofiber fabrication (Figure 4d).[89] The fabrication method is capable of producing oriented fibers, hierarchical cross-linked fibers, and all-in-fiber functionalities thanks to the precise control on the movement of the host templates. However, most of these methods are not capable of large-scale production and need to evolve to adapt to the new generation of materials. One of these materials is liquid crystal elastomer, a material composed of a polymer backbone with attached liquid crystal groups, enabling large deformation in response to external stimuli such as temperature. Extrusion-based fabrication of ultra-fine fibrous structures from liquid crystal elastomers is a major challenge due to the importance of alignment on functioning of these elastomers. To address this issue, melt electrowetting is developed, which is capable of fiber manufacturing with well-defined morphologies by inducing preferential alignment on mesogens of the fiber axis (Figure 4e).[90] Further control on the fiber morphologies can merge with higher production efficiency by combining the traditional fiber spinning methods. Electro-blown spinning is one of the significant advancements that integrate electrospinning and solution blow spinning, realizing nanofiber formation from sustainable, conductive, highly porous, mechanical resilient materials (Figure 4f).[91] These fibers have nanometer sized diameter, but often suffer from minimal control on their other geometric properties such as length. Rotating wet spinning offers a rapid, ultra-long fiber spinning while providing the precise control over fiber morphology realized by the wet spinning process (Figure 4g).[92] Owing to enhanced control on the fiber properties offered by this method, textiles with ballistic and thermal protection are developed for personnel working in extreme conditions. The extreme functionality for these fibers requires unique fiber morphologies, often not feasible by available fabrication methods. Thermal insulating fibers, for example, demand materials with extreme thermal properties that are not often compatible with traditional spinning or printing methods. Freeze spinning offers aligned porous structures for ultra-thin fibers, mimicking natural fibers of polar bear hairs as an animal thriving in extremely cold conditions (Figure 4h).[93] In this method, directional freezing, provided by the yellow ring illustrated in the Figure 4h, is combined with solution spinning to form biomimicking fibers. While fibers with extreme morphologies are feasible through this method, the energy footprint of this method makes it challenging for its widespread application. On the other hand, laser-assisted, melt-blown nanofiber formation provides a facile solution for fiber formation of low viscous materials, thereby reducing the amount of polymer involved, and final cost of their production (Figure 4i).[94] In this

method, lasers radiated on the spinneret increase the temperature of the polymer solution, decreasing its viscosity, and make the produced fibers thinner. Laser-assisted, melt-blow spinning is compatible with large-scale manufacturing, with some promise to significantly reduce the cost for fiber-based products such as facemasks.

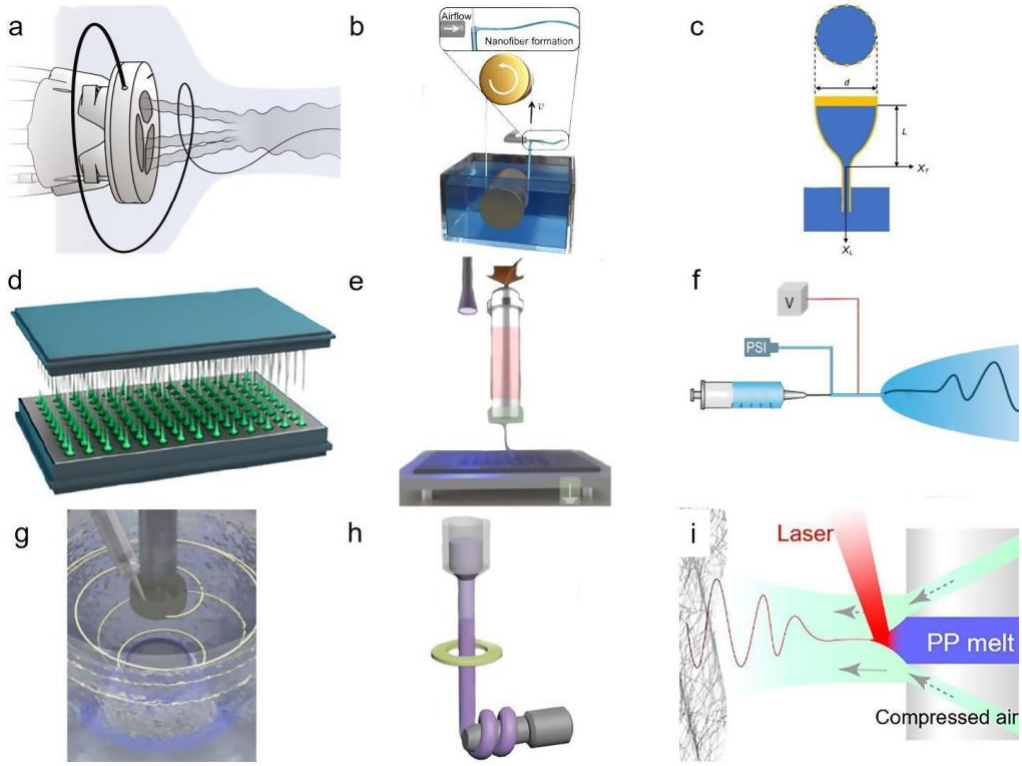

Figure 4. Emerging fabrication methods to produce functional fibers. (a) Usage of air in controlled alignment of fibers produced by rotary jet spinning. Reproduced with permission from Chang et al., Science 377, 180 (2022). Copyright 2022 American Association for the Advancement of Science.[85] (b) Spinning solution on a rolling thread through jetting produced by shear stresses of a high-speed gas flow. Reproduced with permission from Li,et al., Sci. Adv. **8**, eabn3690 (2022); licensed under a Creative Commons Attribution (CC BY) license.[87] (c) Schematics of elastocapillary production of fibrous structures Reproduced with permission from Guan et al., Sci. Adv. 5, eaav2842 (2019). Copyright 2019 American Association for the Advancement of Science.[88] (d) Schematics of capillary-control fiber spinning. Reproduced with permission from Ni et al., Nano Lett. 22, 9396 (2022). Copyright 2022 American Chemical Society.[89] (e) Schematic illustration of melt electrowriting. Reproduced with permission from Javadzadeh et al.,Adv. Mater. e2209244 (2022). Copyright 2022 John Wiley and Sons.[90] (f) Schematics of an electro-blown

spinning setup, a hybrid manufacturing setup consisting of electrospinning and solution blow spinning. Reproduced with permission from Cao et al., Adv. Mater. 33, e2102500 (2021). Copyright 2021 John Wiley and Sons.[91] (g) Schematics design of immersion rotary jet-spinning platform. Reproduced with permission from Gonzalez et al., Matter 3, 742 (2020). Copyright 2020 Elsevier.[92] (h) Schematics of freeze spinning, a combination of directional freezing with solution spinning methods. Reproduced with permission from Cui et al., Adv. Mater. 30, e1706807 (2018). Copyright 2018 John Wiley and Sons.[93] (i) Schematics of laser-assisted solution blow spinning setup. Reproduced with permission from Yang et al., Nano Lett. 22, 7212 (2022). Copyright 2022 American Chemical Society.[94]

The development of new platforms that can evolve and adapt to large-scale industrial processes and produce consistent fibers remains a crucial area of focus. Among the emerging processes, rotary jet spinning and roller jetting have shown great promise in producing fibers rapidly and on a large scale compared to other emerging platforms for fiber production, but more analysis is required to determine their consistency. Template-assisted fiber production, on the other hand, offers excellent control over fiber size and morphology, although scaling up these fabrication methods poses significant challenges. Emerging platforms that combine established fiber production methods, such as melt electrowriting, offer the advantages of conventional methods with added benefits, but further development is necessary to achieve rapid and scalable fiber production suitable for real-world fabric and textile applications.

3. Platforms

Recent advances in manufacturing techniques have enabled the production of high-performance fibers. Therefore, platforms have become critical for maintaining continuous contact between fibrous wearable and implantable devices and human tissues both on and inside the body. We have reviewed the advances in developing these platforms within two main, broad categories: (i) conductive fibrous bioelectronics and (ii) their integration pathways into a functioning biomedical device.

3.1 Conductive fibrous bioelectronics

Fibers in the bioelectronic devices are essential to allow electrons flow through the device, enabling these fibrous devices to transmit, process, and store information.[95] Fibers can facilitate the flow of electrons through the use of conductive materials either embedded within them,

composed entirely of them, or coated with conductive agents. Fibers with core/sheath structure is an ideal platform to contain conductive materials (Figure 5a-left), enabling highly conductive fibers by using flowable conductive materials such as eutectic gallium-indium (EGaIn). These fibers are stretchable and maintain stable conductance in extreme mechanical deformations (Figure 5a-right).[53] Apart from containing conductive materials inside fibers, coating of metallic and conductive materials, such as gold (Au) or silver , on the fibrous substrates is another facile, easy-to-use method to realize breathable, porous electronic devices (Figure 5b).[96] Cleanroom processes, e.g., vapor deposition,[96] sputtering,[97] and spin coating,[98] are also capable of depositing thin conductive films on fibrous sensors, enabling acquisition of high quality, high-fidelity biomedical signals (Figure 5c).[96] Mixing conductive agents such as metallic nanowires and nanoparticles provides another facile method to impart electrical conductivity to often insulating polymeric fibers (Figure 5d).[99–107] These conductive elastomers are also capable of remaining conductive under cyclic loads of mechanical deformation, realizing durable, conductive fibers (Figure 5e).[100] To enhance the mechanical stability of fibers, the alignment of the conductive materials inside the fibers also plays an important role. The degree of alignment for these often small, conductive nanoparticles and nanowires is controlled during the spinning process. For example, fibers made from gold nanowires with higher degree of alignment realize mechanically strong fibers (Figure 5f & g).[108] To simplify manufacturing processes of conductive fibers and potentially reduce the costs and chemical waste through the process, fabricating fibers purely from conductive materials offers a single-step solution for facile manufacturing of functional fibers and minimizing the associated costs for their fabrication. There are a variety of conductive materials compatible with available fiber spinning and fiber printing processes ranging from 1D & 2D materials like MXene (Figure 5h & j),[60,109] Graphene (Figure 5l & m),[110–113] and Carbon nanotube (CNT, Figure 5p)[74] to conductive polymers such as poly(3,4-ethylenedioxythiophene) polystyrene sulfonate (PEDOT:PSS, Figure 5n).[114] Fibers are fabricated purely from conductive 2D materials primarily through wet/dry spinning. One of the emerging classes of 2D materials is MXene, a promising material with exceptional electroconductivity and electrochemical properties.[115,116] MXene fibers are capable of performing electrochemical analysis with broad peaks for the H^+ intercalation/deintercalation and surface redox (Figure 5i) while exhibiting a strong mechanical stability and elasticity (Figure 5k).[109] Graphene is another exciting 2D material, gaining staggering attention in the recent decade due its unprecedented electrical conductivity,[117] thermal

properties,[118] and mechanical strength.[119–122] Graphene has higher electrical conductivity, mechanical strength, thermal conductivity, and surface area over other emerging 2D materials such as MXene, calling for their wide range of applications in different shape form factors. Fibrous form of graphene, realized primarily by wet spinning, is an excellent substrate to controllably attach to a variety of additives, enhancing their sensory performance to the surrounding physical and chemical signals (Figure 5l).[110] These 2D materials, however, are not easy to handle as they are often not stable in a broad range of physicochemical properties.[123–125] Conductive polymers are another class of organic materials with metal-like properties and flexibility of polymers, capable of conducting electricity typically due to the presence of conjugated functional groups in their structure.[126] The exceptional processability of this class of materials makes them highly suitable for the formation of conductive fibers. For example, PEDOT:PSS fibers can successfully be spun by wet spinning process, potentially capable of removing insulating PSS components and further increasing the electrical conductivity of the fiber (Figure 5n).[114] Precise control over polymer aggregation during the wet spinning process of PEDOT:PSS fibers results in the creation of stronger and more stretchable fibers, which are ideal for use in wearable and implantable biomedical devices (Figure 5o).[114] PEDOT:PSS is considered a quasi 1D material with percolating filament network of conductive wires. One-dimensional materials typically exhibit superior mechanical properties compared to 2D materials, making them a more suitable option for flexible devices due to their increased resistance to mechanical stresses, such as bending or buckling, resulting from their higher aspect ratio. This makes them attractive candidates for the growing field of flexible bioelectronics. CNTs are emerging as a promising class of one-dimensional materials with increasing biomedical applications, attributed to their facile surface functionalization, biosensing capabilities, and inherent chemical stability. CNT fibers can be made with tunable mechanical properties dependent on the fibers winding rate and the nanotube alignment.[127] The excellent alignment of CNT is currently available through simple manufacturing methods such as direct writing (Figure 5p).[74] Due to the excellent electrical conductivity, CNT fibers can also provide reliable energy resources and integrate into contact-based energy generation (Figure 5q & r).[74]

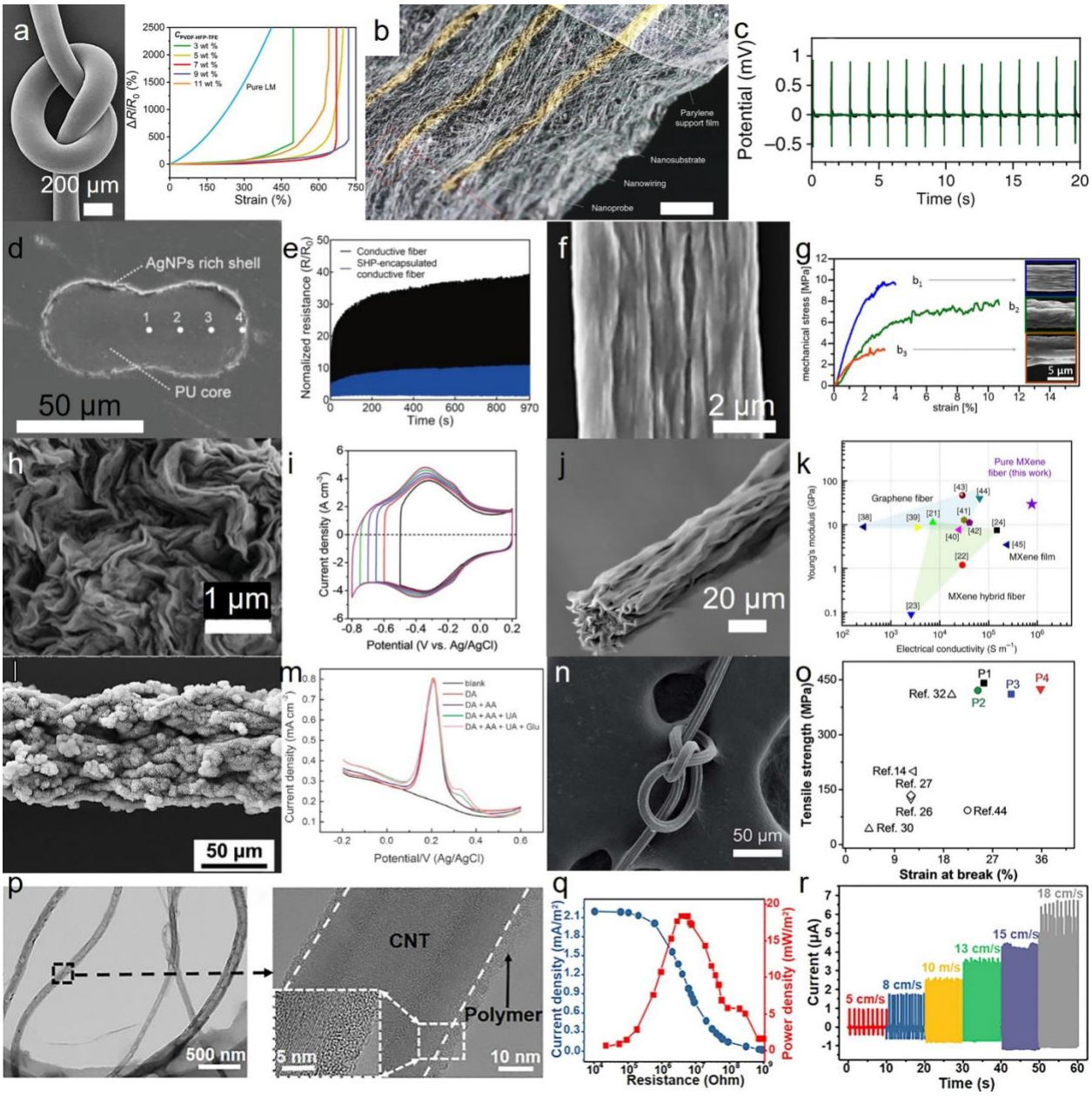

Figure 5. Electroconductive fibers. (a) a snapshot of knotted core/sheath microfiber made of PVDF-HFP-TFE shell and liquid metal core (left) and its conductance stability in mechanical deformation up to ~700% stretchability (right). Reproduced with permission from Zheng et al., Sci. Adv. 7, eabg4041 (2021). Copyright 2021 American Association for the Advancement of Science.[53] (b) Optical image of electrospun substrate with gold deposited electrodes. Scale bar, 2mm. (c) Field potentials of cardiomyocytes using electrospun fibrous electrodes coated with a thin film of gold. B-c, Reproduced with permission from Lee et al., Nat. Nanotechnol. 14, 156 (2019). Copyright 2019 Springer Nature.[96] (d) SEM cross-sectional image of a conductive,

stretchable fiber, made with a butanol-based material. (e) The endurance of cyclic stretching for a conductive fiber (black) and a conductive fiber encapsulated with a tough self-healing polymer (blue). D-e, reproduced with permission from Kwon et al., Adv. Funct. Mater. 30, 2005447 (2020). Copyright 2019 John Wiley and Sons.[100] (f) Au nanowire fibers fabricated by wet spinning. (g) Stress-strain curve exhibiting the effect of nanowire alignments on the mechanical strength of the fiber. F-g, Reproduced with permission from Reiser et al., ACS Nano 11, 4934 (2017). Copyright 2017 American Chemical Society.[108] (h) Cross section of a PEDOT:PSS/MXene fibrous composite. (i) cyclic voltammetry (CV) profiles of MXene/PEDOT:PSS composite fibers, obtained at different operational potentials and a scanning rate of 5 mV s^{-1}. h-i, Reproduced with permission from Zhang et al., Small 15, e1804732 (2019). Copyright 2019 John Wiley and Sons.[109] (j) SEM image of pure MXene fiber. (k) Comparison of electrical conductivity and Young's modulus of pure MXene fiber. J-k: reproduced with permission from Eom et al. Nat. Commun. **11**, 2825 (2020); licensed under a Creative Commons Attribution (CC BY) license.[60] (l) SEM image of graphene fiber with nickel-cobalt phosphide nanosheet arrays, realized by solvothermal reaction in metal precursor solution. (m) Different pulse voltammetry responses of graphene fiber with nickel-cobalt phosphide nanosheet arrays with 100 μM dopamine (red) in the presence of 500 μM ascorbic acid (blue line), 500 μM ascorbic acid and 500 μM uric acid (green line), and 1.0 mM ascorbic acid, 1.0 mM uric acid and 1.0 mM glucose (purple line). l-m: reproduced with permission from Zhao et al., Biosens. Bioelectron. 205, 114095 (2022). Copyright 2022 Elsevier.[110] (n) SEM snapshot of PEDOT:PSS fiber. (o) Maximum tensile strength of the PEDOT:PSS fibers and comparison with other fibers including graphene fibers. N.o. Reproduced with permission from Zhang et al., J. Mater. Chem. A Mater. Energy Sustain. 7, 6401 (2019). Copyright 2019 Royal Society of Chemistry.[114] (p) Transmission Electron microscopy image of CNT fibers, exhibiting a good dispersion of CNT within the fiber. (q) The relationship between the resistance of a 3D-printed smart textile made from CNT fiber and its output short-circuit current and power density. (r) Measurements for the output short-circuit current generated by a grid line pattern on a textile as it comes into contact with or separates from a PET film at varying displacement speeds (5, 8, 10, 13, 15, and 18 cm s^{-1}). p-q: reproduced with permission from Zhang et al., Matter 1, 168 (2019). Copyright 2019 Elsevier.[74]

3.2 Fibrous platforms

Wearable and implantable fibrous devices require platforms that are conformable, affordable, and safe to use. Among numerous ways to integrate fibers into functional biomedical devices, we have characterized readily available platforms such as masks (Figure 6a),[74] accessible fibrous materials like papers (Figure 6d),[128–130] thin self-standing fibrous stickers (Figure 6g),[131–133] and fibrous textile (Figure 6j)[134] as the promising pathways to use fibers in the biomedical devices. Fibers inside masks exhibited high performance air filtering down to 0.3 μm particles (Figure 6b),[135] exploiting electrostatic adsorption and triboelectrification to increase the lifespan of the mask (Figure 6c). To enhance the integration of fibers into readily available platforms, materials are also playing a paramount role in engineering the fibrous material properties and compatibility with wearables and implants. Paper, made from cellulose fibers, is a highly accessible fibrous substrate with a wide range of properties, including a broad range in fiber diameter and density. By simply using a conductive paste such as silver flakes, cellulose fibers transform to highly conductive substrates capable of induction heating (Figure 6e)[128] and wireless power transmission (Figure 6f).[128] While papers are breathable, cost-effective, and biocompatible electronic substrates, there are remaining challenges in interfacing their hygroscopic surfaces with wet biological tissues. One of the possible ways to circumvent this problem is to use thin nanofibrous substrate made by electrospinning to act as an interface between thin metallic films and the biological tissues (Figure 6h).[133] These fibers are often also used as a transferring platform that can be dissolved once on top of the skin. Polyvinyl alcohol (PVA) fibers are one of the ideal candidates to transform thin metallic films as a sacrificial layer owing to their solubility in water. They can place fibrous electronics onto the skin, providing the necessary adhesion to the tissue and intimate contact with the skin (Figure 6i).[133] Fibers can also seamlessly weave into textile structures, as demonstrated in Figure 6j.[134] By utilizing molded building blocks, it is possible to fabricate power sources such as batteries using intricate fiber structures (Figure 6k and l).[134] These fibrous batteries have stable cycling performance exceeding long hours and minimal capacity drops over repetitive charging/recharging processes. These advancements pave the way towards fibrous digital platforms capable of measurement, processing, and transferring information with prolonged functioning thanks to robust batteries.

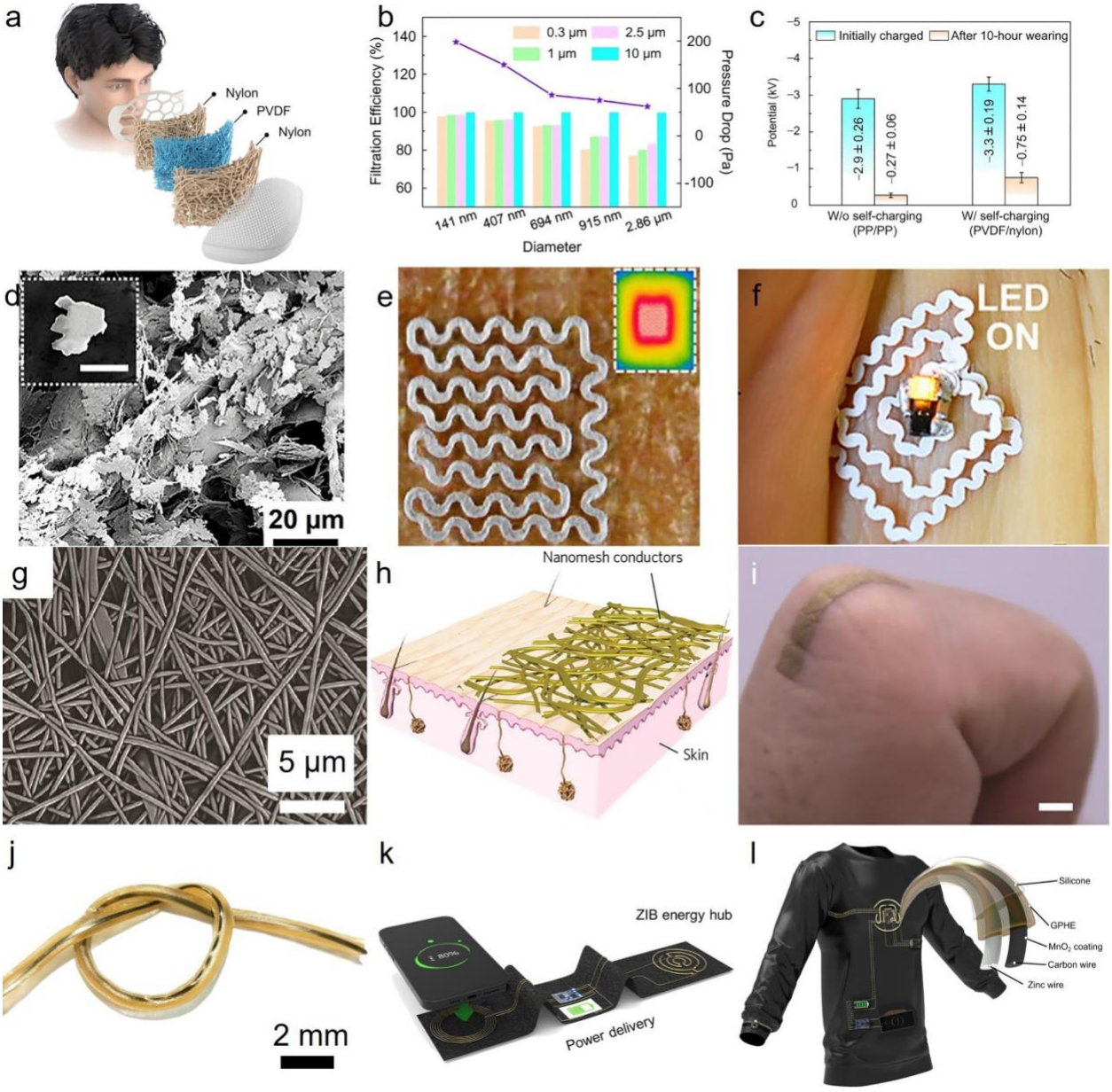

Figure 6. Fibrous platforms for wearable and implantable bioelectronics. (a) A diagram outlining the design of the self-charging mask. (b) The effect of fiber diameter on filtration efficiency and pressure drop. (c) the difference in electrostatic potential reduction between the self-charging and non-self-charging masks. The presented data represents the mean values with standard deviations, based on five independent samples. a–c, reproduced with permission from Peng et al., Nat. Commun. 13, 7835 (2022); licensed under a Creative Commons Attribution (CC BY) license.[135] (d) Silver microflakes deposited on cellulose fibers and their full integration to (e) wireless heater and (f) wireless optical neurostimulators. Reproduced with permission from Sadri

et al., ACS Appl. Mater. Interfaces 10, 31061 (2018). Copyright 2018 American Chemical Society.[128] (g) SEM image of nanomesh conductor made from polyvinyl alcohol (PVA). (h) A schematics of laminated gold film on the electrospun PVA fibers. (i) Seamless integration of nanomesh conductors on the finger skin. g-i, reproduced with permission from Miyamoto et al., Nat. Nanotechnol. 12, 907 (2017). Copyright 2017 Springer Nature.[133] (j) An optical image of zinc ion fibrous batteries (ZIB) with graphene oxide embedded PVA hydrogel electrolytes. (k) Wireless power transfer between a smartphone and ZIB fibers using textile-based technology. (l) A design for wireless textile body area network. j–l, reproduced with permission from Xiao et al., Sci. Adv. 7, eabl3742 (2021). Copyright 2021 American Association for the Advancement of Science.[134]

4. Applications

The success of wearable and implantable biomedical devices depends largely on their ability to perform their intended function, which is highly dependent on their applications. In this section, we explore the importance of applications for fibrous wearable and implantable devices, focusing on five key categories: power sources, thermal management platforms, sensors, electrophysiological recording, and electrostimulation. These applications play a crucial role in optimizing the functionality and performance of fibrous devices, as well as their overall safety and efficacy. By examining the latest advancements in each category of application, we aim to provide valuable insights into the development and optimization of fibrous wearable and implantable devices.

4.1 Power management using fibrous electronics

Wearable and implantable devices are increasingly capable of multiplexed sensing and monitoring a range of biosignals from heart to brain activity. The rapid advancements in the functioning of these biomedical devices demand versatile, wireless, and self-powered energy resources.[130,136,137] The fibrous platforms promise the next generation of energy resources thanks to their large surface area and their compatibility with modular designs. Triboelectric nanogenerator is one of the emerging platforms woven with fibers, harvesting mechanical energy to provide self-powered energy.[138] In this method, two materials with different electronegativity come in contact and then separate, leading to electron transfer between them (Figure 7a).[74] Multimaterial fibers with several liquid metal cores can form an all-in-fiber triboelectric system, capable of producing electrical output up to 490 V, 175 nC (Figure 7b),[48] and easily integrate to daily fibrous products such as

textiles. Apart from multi-material fibers, multilayer fibrous designs are also able to produce triboelectric signals, exploiting them for both energy demands and sensing purposes (Figure 7c).[48] Triboelectric energy generation is not the only way to harvest and transform mechanical energy to electrical energy. Piezoelectric materials such as quartz, lead zirconate titanate, or gallium phosphate are also able to transform mechanical pressure, tension, or vibration to electrical signals. Piezoelectric polymers such as polyvinylidene fluoride (PVDF) and polyethylene terephthalate (PET) are a class of piezoelectric materials, compatible with traditional fiber manufacturing methods, and are the predominant building materials for piezoelectric fibers (Figure 7d).[139] Piezoelectric fibers can be effectively blended with other piezoelectric materials to increase the electrical response for a given mechanical energy input (Figure 7e).[139] The mechanical disturbances of piezoelectric fibers generate rapid response through the fiber possibly due to instantaneous creation of dipole moment along the constituent molecules of piezoelectric polymer (Figure 7f).[139] While self-powered devices are of paramount importance in supporting the performance of the biomedical devices, energy storage platforms are also necessary for prolonged, sustainable use of these devices. Batteries as one of the well-known energy storage systems are experiencing tremendous advancements in the recent few decades, perfectly adopting the flexible, lightweight nature of wearables and implants. These energy systems are advanced enough to integrate into fibrous textiles (Figure 7g),[140] and get their energy from different resources such as solar, biofuel, or thermal energy. The performance of batteries is closely dependent on the type of energy resource they get their energy from. For example, the efficiency of fibrous batteries made from photosensitive materials such as perovskite–TiO2–carbon fibers is subjected to the wavelength of the light available for these devices (Figure 7h).[141] These devices can easily intertwine into textiles, providing the energy to charge devices like smartphones by simply using the energy from the surrounding light (Figure 7i & j).[140,141] The need for faster, power-efficient, powerful computing in biomedical devices heralds generation of devices in mini and microscales. Fibrous energy platforms are no exception, and they experience significant improvement in minimizing the scale of fibers for energy production and storage. As demonstrated in Figure 7k,[142] one of the possible ways is to merge energy generation and storage into a single fiber. Carbon fibers surrounded by Poly(vinylidene fluoride-co-hexafluoropropylene) polymers (PVDF-HFP) exhibit a rectangular curve, an ideal energy storage platform to store energy in the double layer of the electrode (Figure 7l).[142] The mechanical stability of these fibers make them an ideal candidate

to retain capacitance and power while bending, knotting, and washing (Figure 7m) while demonstrating power generation and application potential while attached to the daily clothing (Figure 7n).[142] To ensure the dissemination of fibrous platforms into the market, it is necessary to move beyond single fiber engineering and move toward scalable manufacturing techniques. Fiber batteries with anode and cathode within their structure, manufactured through a wet spinning process, offer scalable, compact, and wearable power solutions (Figure 7o).[143] The large-scale production of these fibers have made it possible to fabricate large scale textiles and enhance their absolute discharge capacity to roughly 40 mAh for a 1,000 cm2 textile battery (Figure 7p).[143] Their practical applications are even extended to power a smart soundbox and a textile display as shown in Figure 7q.[143]

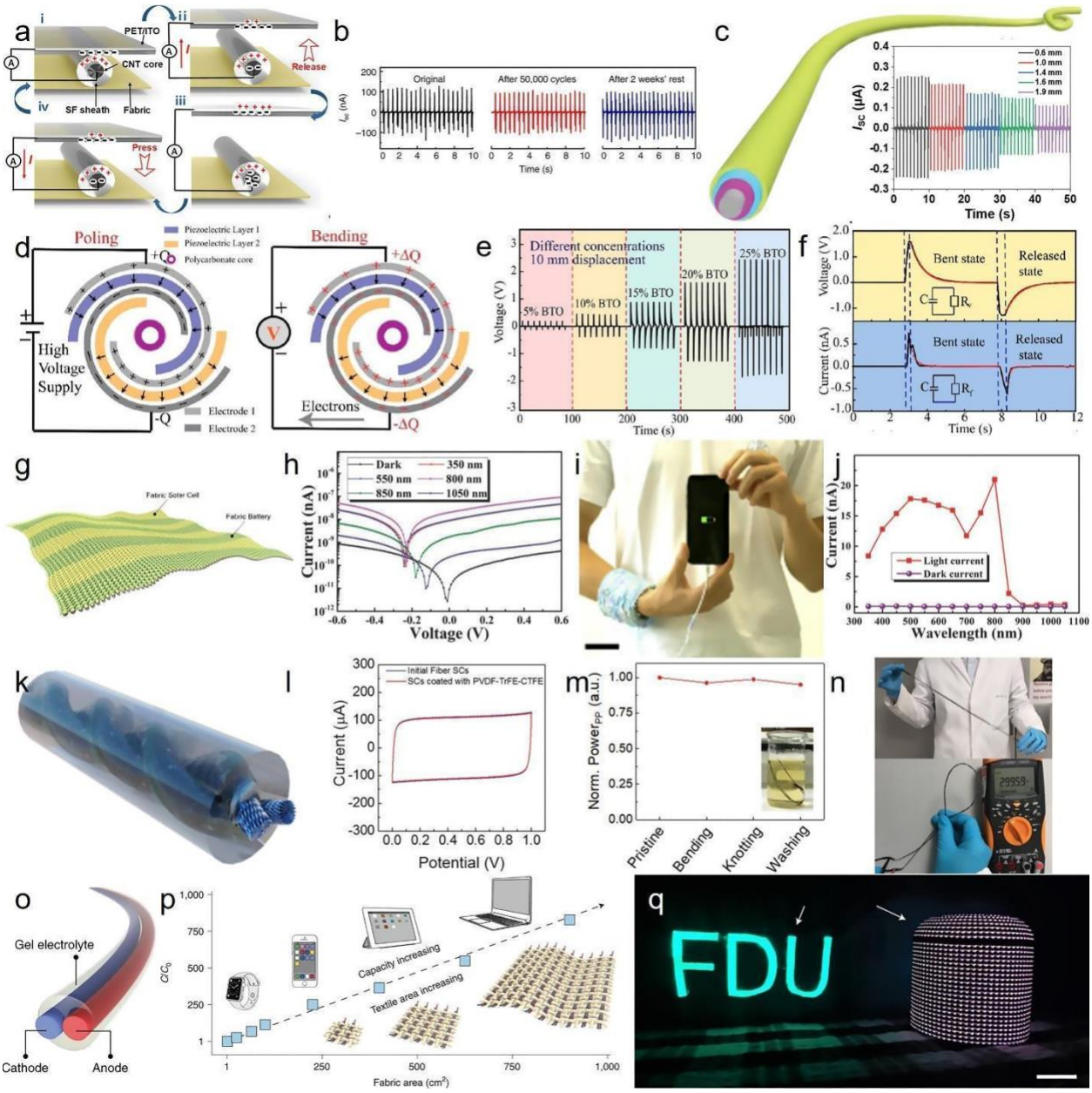

Figure 7. Power management using fibers. (a) Schematic illustration of the working mechanism for fiber-based triboelectric nanogenerators (TENG). Reproduced with permission from Zhang et al., Matter 1, 168 (2019). Copyright 2019 Elsevier.[74] (b) Output evaluation and long-term stability of TENG fibers after subjecting it to continuous pressing for 50,000 cycles, and being stored in the ambient atmosphere for 2 weeks (contact length: 3 cm). (c) Schematics illustration of multi-layer TENG fibers. b,c, Reproduced with permission from Dong et al. Nat. Commun. 11, 3537 (2020); licensed under a Creative Commons Attribution (CC BY) license.[48] (d) Schematics of power generation through piezoelectric fibers. (e) open-circuit voltage produced by a BaTiO3-

poly(vinylidene fluoride) fiber that is 10 cm long and has varying BaTiO3 concentrations (5%, 10%, 15%, 20%, and 25% by weight) when subjected to a 1 cm displacement. (f) Open-circuit voltage and short-circuit current of the piezoelectric fiber, measured during its bending and releasing actions. d–f, Reproduced with permission from Lu et al., ACS Nano 11, 2103 (2017). Copyright 2017 American Chemical Society.[139] (g) Schematic diagram of photo-rechargeable fibrous battery. Reproduced with permission from Zhang et al., Matter 2, 1260 (2020). Copyright 2020 Elsevier.[140] (h) Current-voltage curve of the photodetector, obtained under different wavelengths of light and in darkness. Reproduced with permission from Sun et al., Adv. Mater. 30, e1706986 (2018). Copyright 2020 John Wiley and Sons.[141] (i) Charging a cell phone using photo-rechargeable fabrics. Reproduced with permission from Zhang et al., Matter 2, 1260 (2020). Copyright 2020 Elsevier.[140] (j) Dependence of photocurrent and dark current on different wavelengths of irradiated light. Reproduced with permission from Sun et al., Adv. Mater. 30, e1706986 (2018). Copyright 2020 John Wiley and Sons.[141] (k) Schematic demonstration of a fibrous supercapacitor. (l) CV curve for a fibrous supercapacitor with scan rate of 10 mV s^{-1} from 0 to 1 volt. (m) Stable power generation of fibrous supercapacitor under a variety of mechanical stresses. (n) Potential charged in fibrous supercapacitors and their integration at scale. k–n, Reproduced with permission from Cho et al., Adv. Funct. Mater. 30, 1908479 (2020). Copyright 2020 John Wiley and Sons.[142] (o) Schematics of three-component extruded battery. (p) Linear increase for discharge capacity of fibrous energy storage textile with fabric area. (q) Powering textile display (left) and smart sound box (right) using textile batteries. o–q Reproduced with permission from Liao et al., Nat. Nanotechnol. 17, 372 (2022). Copyright 2022 Springer Nature.[143]

4.2 Thermal management using fibers

The most common wearable device is fibrous textile- a breathable, soft, and lightweight platform worn by almost everyone daily for several centuries. One of the most prominent functions of these fibrous platforms is to provide comfort for the user by protecting them from thermal irregularities of the environment. Over the years, with a new generation of advanced materials and sophisticated fabrication techniques, control over fiber morphologies and its form factors has experienced tremendous improvement. The level of control on the fiber formation has resulted in producing biomimetic fibers for thermal management with comparable performances to their naturally evolved ones. For example, polar bears can survive through the harsh winters thanks to their hollow hairs made from collagen protein. Inspired by their excellent thermal insulation properties,

fibers made from silk fibroin can mimic passive insulating heat loss due to the poor thermal conductivity of trapped air within the core of their core/shell structure (Figure 8a).[93] These fibers are also suitable for large-scale knitting systems and can be incorporated into textiles (Figure 8b).[93] The insulation efficiency for the textile is generally defined by the temperature difference between the heat source and the surface of the textile fiber. For silk fibroin porous fibers, the temperature difference is higher with increasing the porosity of the produced fibers (Figure 8c).[93] Therefore, fibers with higher porosity are better candidates for enhanced thermal insulation. To further improve the thermal stability, nanomaterials such as graphene nanoparticles can be used to mix with silk fibers, realizing fabrication on a large scale (Figure 8d),[91] and resist high temperatures created by flames (Figure 8e).[91] Using weight loss as an indicator for material decomposition in high temperature, produced silk/graphene fibers display a higher resistance in high temperatures compared to pure silk fibers (Figure 8f).[91] Manipulating thermal energy by fibrous platforms is not restricted to fabrication of thermally protecting structures. Transforming thermal energy to other useful forms of energy is another exciting application for the new generation of fibers. Thermoelectric fibers, capable of producing electric voltage from temperature gradients, are offering a realistic solution to exploit thermal energy and power wearable biomedical devices. They can easily integrate to textile thanks to their fibrous structure and scalable manufacturing (Figure 8g & h),[144] and produce electric voltage with temperature differences as low as 5 °C (Figure 8i).[144] Thermal energy transport in these fibers are often studied within the material. However, thermal management processes such as radiative heating provide another opportunity for medium-free, high thermal effect, and good penetration of heat transfer. Some of these fibers can controllably be woven into textile (Figure 8j & k)[145] and are made of mechanical compliant materials such as glass fibers and graphene. The produced fibers show negligible change in emissivity to temperature increase, with the optimum wavelength for maximum radiation efficiency can be achieved by judiciously selecting working temperature (Figure 8l).[145]

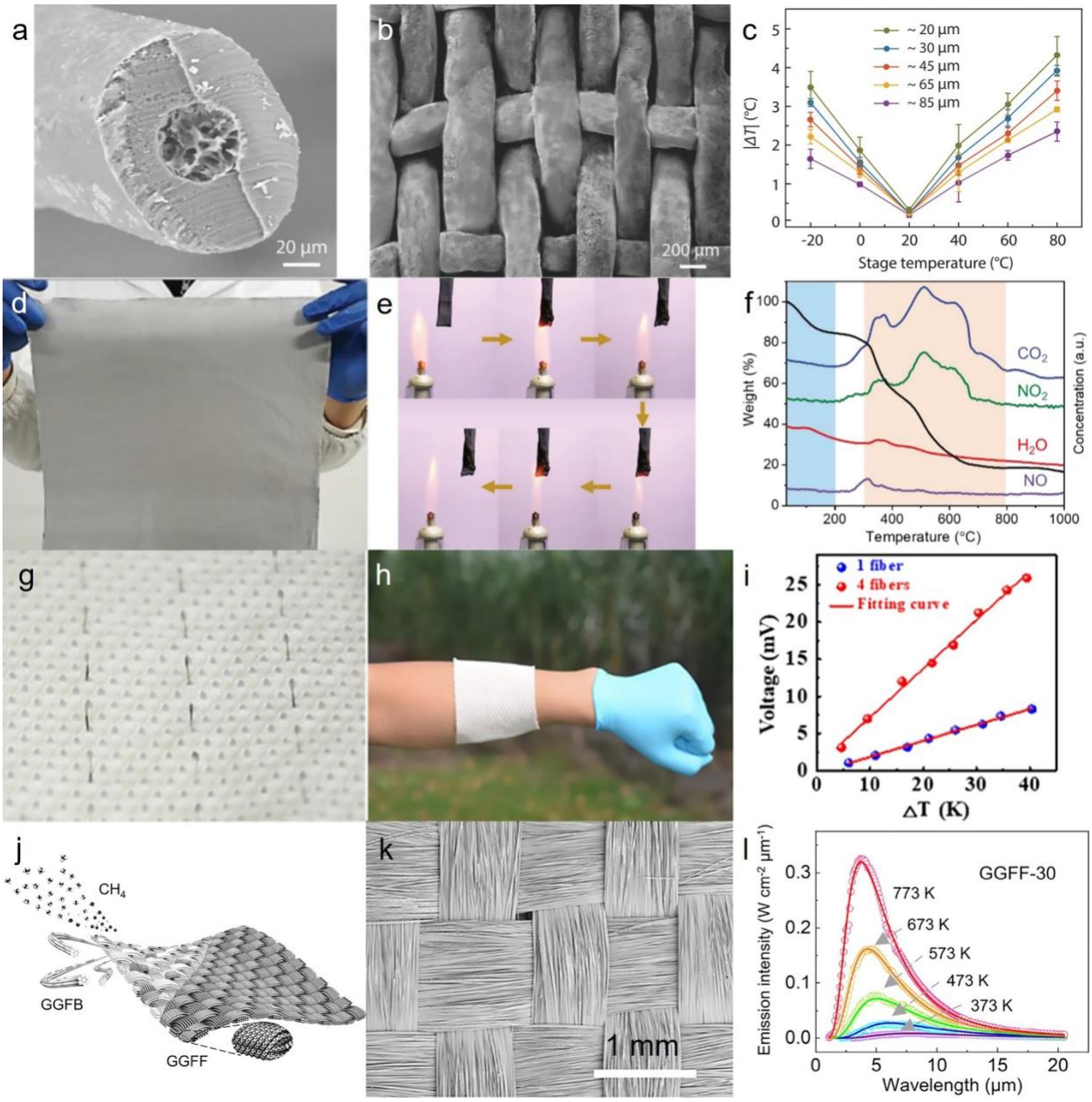

Figure 8. Thermal management using fibers. (a) Cross sectional SEM image of hollow core with aligned shell of a polar bear hair fiber. (b) Woven textile of biomimetic porous fibers made from silk fibroin. (c) The dependence of temperature difference on the pore size of the biomimetic fibers. a–c, Reproduced with permission from Cui et al., Adv. Mater. 30, e1706807 (2018). Copyright 2018 John Wiley and Sons.[93] (d) 30 cm×30 cm eletro-blown silk/graphene nanoiontronic (SGNI) fibrous skin. (e) Flame resistance of SGNI skin. (f) Thermogravimetric analysis of SGNI skin. d–f, Reproduced with permission from Cao et al., Adv. Mater. 33, e2102500 (2021). Copyright 2021 John Wiley and sons.[91] (g) An optical image of a thermoelectric

fabric. (h) A thermoelectric fabric on the skin. (i) The effect of temperature difference on open-circuit potential generated by thermoelectric fibers. g–i, Reproduced with permission from Xu et al., ACS Appl. Mater. Interfaces 12, 33297 (2020). Copyright 2021 American Chemical Society.[144] (j) Schematic of fabrics produced by chemical vapor deposition and made from graphene glass fiber bundles and fabrics. (k) 7 μm graphene glass fibers woven into textile. (l) The dependence of infrared emission spectra at a wide range of temperature. j–l, Reproduced with permission from Yuan et al., ACS Nano 16, 2577 (2022). Copyright 2022 American Chemical Society.[145]

4.3 Fibrous chemical wearable sensors

Wearable and implantable devices are designed to interact with the human body. These devices can incorporate sensory platforms, enabling the monitoring of vital health signals over an extended period of time. Chemical sensors, as one of the important classes of wearable and implantable sensors, are designed to detect chemical or molecular species in a sample with a transducer converting chemical information into a measurable signal. These sensors can quantify a range of chemical information from physiological to environmental signals. Monitoring environmental signals, for instance, helps the user to manage their exposure to dangerous chemicals in the environment and helps them make informed decisions. Gas sensors merged with fibrous textile are ideal platforms to monitor the gas chemical species in the environment. Fibers made from nanocellulose mixed with single-walled carbon nanotubes (SWCNTs) show sensitivity to some pollutant gasses such as NO_2 (Figure 9a).[146] The composite fibers show ohmic contact resistance, exhibiting an excellent contact with contact electrodes and displaying prominence for integration with other devices (Figure 9b).[146] The real-time NO_2 response of graphene oxide/SWCNT fibers is realized possibly due to an increase in hole carrier concentration of CNT as a result of electron transfer to NO_2 (Figure 9c).[146] Humidity is another important environmental signal impacting human health by perspiration rate, hydration level, and respiration systems. Recently, ultra-long fibers made from 2D conductive materials such as graphene are applied for humidity sensing, thanks to embedding water dissociation catalysts such platinum (Pt) nanoparticles (Figure 9d).[147] Nitrogen-doped reduced graphene oxide fibers (nRGO) are deposited on electrodes for relative humidity levels of 6.1–99.9% (Figure 9e).[147] Dynamic resistance of humidity sensors increases with higher levels of surrounding humidity and a function of fiber numbers inside the humidity sensitive transistors (Figure 9f).[147] While gas sensing with fibers offers smart textiles for environment awareness and user safety, chemical information from molecular species in liquid

and solid forms encompasses a broader range of insights into human health. Water, electrolytes, hormones, glucose, and lipids delineate important health information on hydration levels, nerve/muscle function, and immune responses, among others. For example, Glucose is a monosaccharide and an important source of energy for the body. The abnormal level of glucose is a clear indicator of a variety of health conditions such as diabetes, hypoglycemia, and metabolic syndrome. Reduced graphene oxide fibrous transistors mixed polypyrrole nanowires have shown an excellent sensitivity for glucose (Figure 9g).[148] These fibrous transistors are capable of a rapid measurement of glucose levels and exhibit excellent reliability in a buffer solution (Figure 9h & i).[148] The outstanding performance of these sensors are possible with numerous methods of measurement ranging from optical to thermal methods. One of the most promising pathways to analytically measuring chemicals is to exploit their electrical properties, often known as electrochemical methods. To perform electrochemical methods, fibers with counter, reference, and working electrodes are fabricated with thermal drawing in a large scale (Figure 9j & k).[149] The effectiveness of these fibers are also evaluated using cyclic voltammetric measurements for a common anesthetic drug called paracetamol (APAP). A linear increase in peak current with higher concentrations of APAP in the buffer solution shows the sensitivity of these fibers comparable with commercially available screen-printed electrodes (Figure 9l).[149]

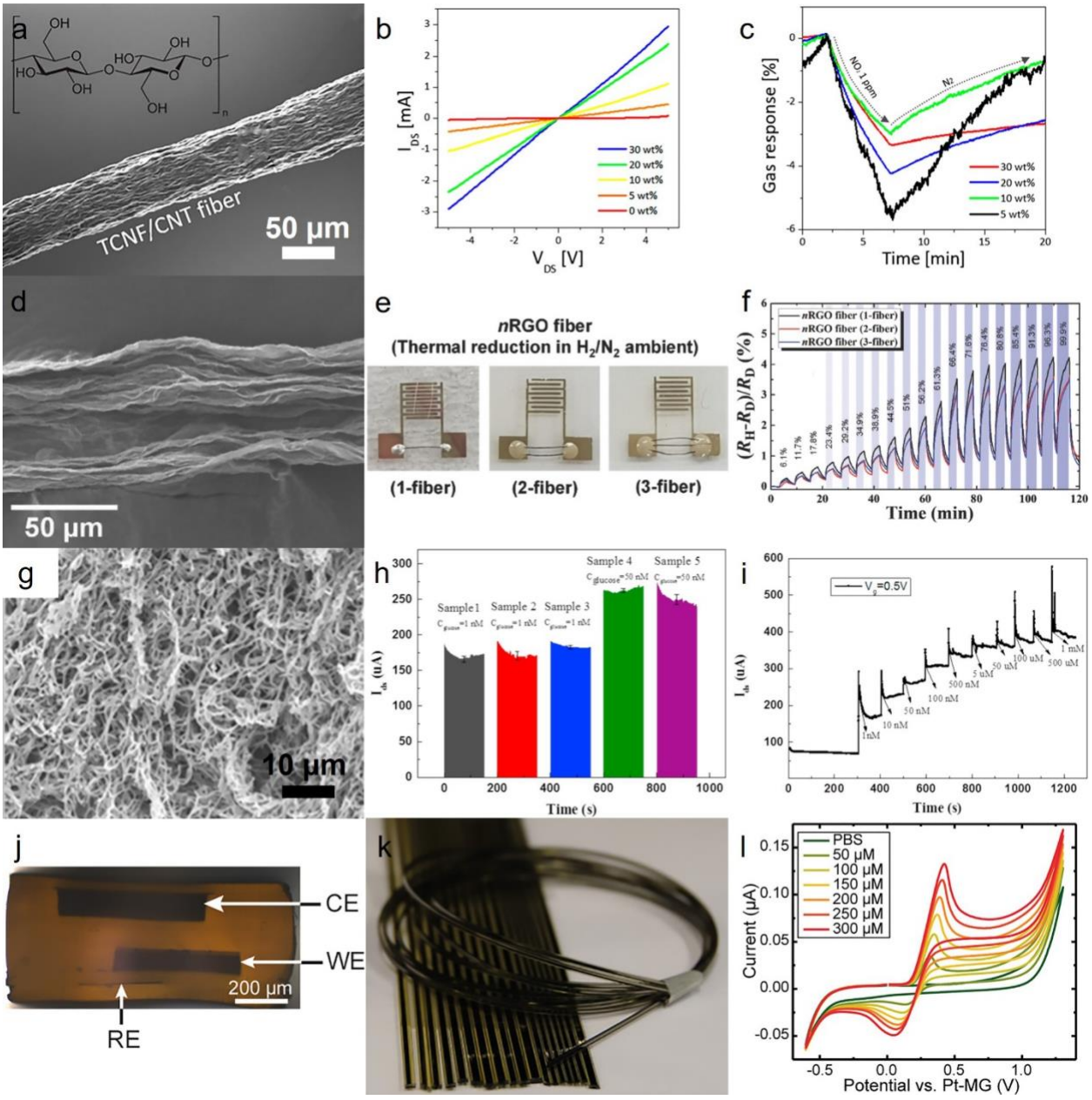

Figure 9 Fibrous wearable chemical sensor. (a) SEM image with low magnification of nanocellulose extracted from tunicate and CNT composite fiber. (b) Current-voltage curves obtained from fibers with a variety of CNT concentration. (c) Real-time NO2 sensing for fibers with different concentrations of CNTs. a–c, Reproduced with permission from Cho et al., ACS Nano 13, 9332 (2019). Copyright 2019 American Chemical Society.[146] (d) Cross section of nitrogen-doped reduced graphene oxide (nRGO) fibers. (e) Optical microscopy image of humidity sensing using nRGO fibers. (f) Humidity sensing using nRGO fibers mixed with platinum nanoparticles. d–f, Reproduced with permission from Choi et al., Small 14, e1703934 (2018).

Copyright 2018 John Wiley and Sons.[147] (g) Magnified SEM images of reduced graphene oxide fibers mixed with polypyrrole nanowires. (h) Repeatability of transistor-based sensing of glucose using fibers. (i) Source-drain current sensitivity of fibrous transistors to different concentrations of glucose. g–i, Reproduced with permission from Wang et al., Biosens. Bioelectron. 95, 138 (2017). Copyright 2017 Elsevier.[148] (j) Optical image of fibers with embedded three electrodes. (k) Scalable production of thermally drawn fibers, capable of electrochemical sensing. (l) Recorded voltammograms of all-in-fiber electrochemical detection of paracetamol at different concentrations. j–l, reproduced with permission from Richard et al., ACS Appl. Mater. Interfaces 13, 43356 (2021). Copyright 2021 American Chemical Society.[149]

4.4 Fibrous wearable physical sensors

Wearable and implantable devices equipped with physical sensory platforms have enabled the continuous and non-invasive monitoring of a range of physiological parameters. Physical sensors are often considered a more reliable platform compared to chemical sensors as they don't need the presence of any specific analytes and are less prone to interference. They have found a wide range of applications from vital signal monitoring to fall detection, closely detecting calories burnt to rehabilitation progress and patient recovery. Integrating physical sensors into fibers allows for even more intimate monitoring, providing increased user comfort and enabling prolonged measurement of health signals. Some of these exciting fibrous physical sensors are exploiting weak physical disturbances and convert them to measurable signals. Magnetoelastic fibers are one of the prominent, emerging examples of these devices, converting the changes in mechanical disturbances to changes in material's magnetic properties. Nanomagnets mixed with silicone polymers are extruded and at the same time heated to form the fibers (Figure 10a).[150] These fibers are highly conductive and display intrinsic water-proofness with a high current density (Figure 10b),[150] enabling measurement of arterial pulses with detection limits as low as 0.05 kPa, even in high perspiration or in underwater situations (Figure 10c).[150] Transduction of mechanical energy to electrical signals is also possible using thermally drawn composite piezoelectric fibers (Figure 10d).[51] A composite fiber made of barium/titanate, PVDF-TrFE, carbon-loaded polyethylene, and copper wire is capable of integrating into textile, draping, and machine washability while acting as an fibrous microphone and acoustic absorber (Figure 10e).[51] The unique properties of piezoelectric composite fibers enable capturing sound waves with applications in sound-direction detection due to its excellent spatiotemporal sensitivity (Figure 10f).[51] Sound waves are not the

only group of mechanical stimuli important for human health monitoring and can expand to low-amplitude and high-amplitude mechanical vibration on the skin, which can relate to heart, muscle, or brain activity. Ultra-thin wearable platforms to capture mechanical disturbances are another promising pathway for using fiber-based biomedical devices. Electrospun nanofibrous platforms made from stretchable materials such as polyurethane-polydimethylsiloxane (PU-PDMS) are coated with thin layers of gold (Figure 10g),[151] realizing durable, ultracomfortable strain sensors to monitor skin deformation of the users (Figure 10h).[151] These breathable electrodes are durable and can fully recover, enabling a prolonged use of these sensors to monitor strain changes on the skin (Figure 10i).[151] These fibrous networks offer a wide range of outstanding sensory performance including pressure sensing and monitoring. Fibrous networks fabricated through electrospinning are made from a polymer solution containing fluorinated copolymer, vinylidenefluoride-tetrafluoroethylenehexafluoropropylene, CNT, graphene, and 4-methly-2-pentanone to form a conductive network (Figure 10j).[152,153] These fibers are transparent, can attach to any surfaces, and monitor applied pressure as low as ~0.6 kPa through an integrated sensory array (Figure 10k).[152] These sensors can operate in low voltage, maintain high sensitivity and measure normal pressure on soft surfaces thanks to their ultra-thin, bending insensitive structures (Figure 10l).[152]

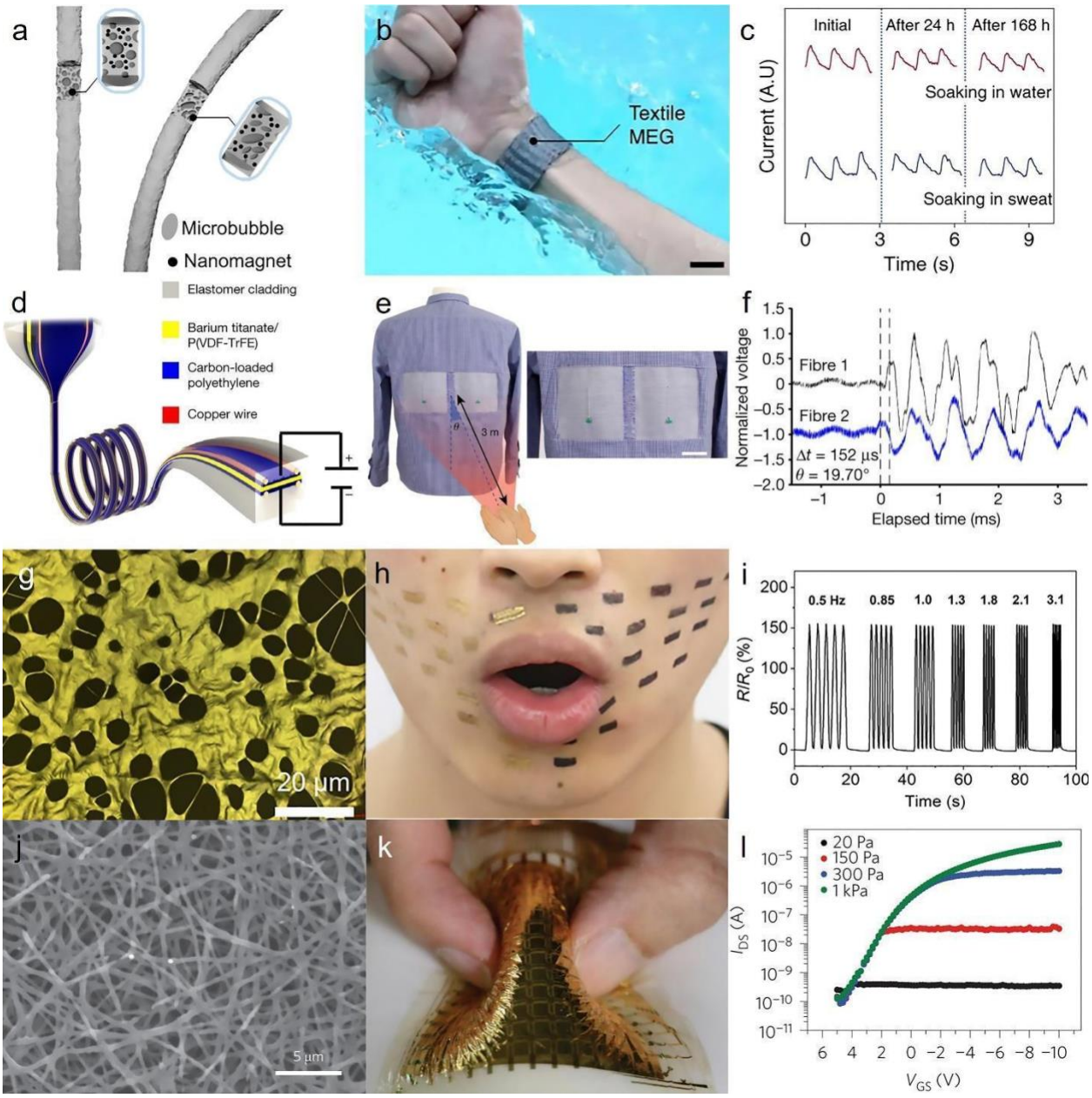

Figure 10 Fibrous wearable physical sensor. (a) Schematic illustration of soft magnetic fiber. (b) Integration of soft magnetic fibers into a wristband. (c) Soft magnetic fibers monitor pulse activity during training or underwater. a–c, Reproduced with permission from Zhao et al., Nat. Commun. **12**, 6755 (2021); licensed under a Creative Commons Attribution (CC BY) license.[150] (d) Schematics of thermal drawing of fiber poling of fibrous microphones. € Integration of fibrous microphones into textile. (f) Thermally drawn fibers capable of spatiotemporal sensitivity. d–f, Reproduced with permission from Yan et al., Nature 603, 616 (2022). Copyright 2022 Springer Nature.[51] (g) Microscopic image of nanomesh composed of polyurethane-polydimethylsiloxane

(PU-PDMS) fibers, laminated with gold. (h) nanomesh seamless integrated on the skin. (i) cyclic stretching/releasing at 30% strain for strain sensors made of PU-PDMS/gold nanomesh. These nanomesh conductors exhibit repeatable and reliable strain measurements. g–i, Reproduced with permission from Wang et al., Sci. Adv. 6, eabb7043 (2020). Copyright 2020 American Association for the Advancement of Science.[151] (j) Field emission scanning electron microscopy image of pressure sensor made from electrospun fibers with random orientation. (k) An optical image of an integrated sensor array on a soft, elastic substrate. (l) I-V response of one pixel array made from electrospun fiber mixed with graphene and CNT at different applied pressure. j–l, Reproduced with permission from Lee et al., Nat. Nanotechnol. 11, 472 (2016). Copyright 2016 Springer Nature.[152]

4.5 Implantable fibrous sensors

Fibers have emerged as a highly suitable platform for monitoring chemical activity inside the body due to their excellent flexibility and miniaturized structures. Implantable fibrous sensors have been used to monitor various crucial biomarkers such as lactate, dopamine, and glutamate, which are effective biomarkers in detection and progression of chronic diseases, metabolic, and neurometabolic disorders.[3,4,154] Owing to excellent mechanical compatibility, fibers are used as a substrate for in-situ monitoring of chemicals within the brain, as one of most sensitive organs to implants.[155,156]

Fibers predominantly made from carbon are traditionally used to monitor neurotransmitters due to their biocompatibility, well characterized electrochemical properties, and excellent sensitivity.[157] Introduced by Pujol and colleagues nearly 50 years ago, carbon fibers are used to measure dopamine, norepinephrine, and serotonin.[158] Detection of non-electroactive compounds can also be possible by using enzyme-based deposition of chemicals on carbon fibers.[159,160] Surface treatment of carbon fibers enables higher sensitivity for the chemical sensors by either enhancing the active surface area or imparting stable conductive connection between the carbon fiber electrode and neighboring tissue.[161–164] Materials such as diamond increases the capacity of the carbon fiber, leading to lower interfacial impedance and higher charge injection capacity (Figure 11a and b).[165] These coatings realize sensitive detection of uric acid and dopamine changes at a single neuron level (Figure 11c).[165] The rapid detection of the compounds are realized using fast-scan cyclic voltammetry (FSCV),[164,166] amperometry,[167] and chronoamperometry[168] for

measurement of both oxidative and reductive currents. Fabrication of fibers with embedded cavities for electrodes and microfluidic channels realize potentiometric and amperometric detection of chemicals inside the body within a single fiber (Figure 11d and e).[169] For example, fibers made from polycarbonate, polyethylene and graphite are capable for in-situ monitoring of lactate inside the brain (Figure 11f).

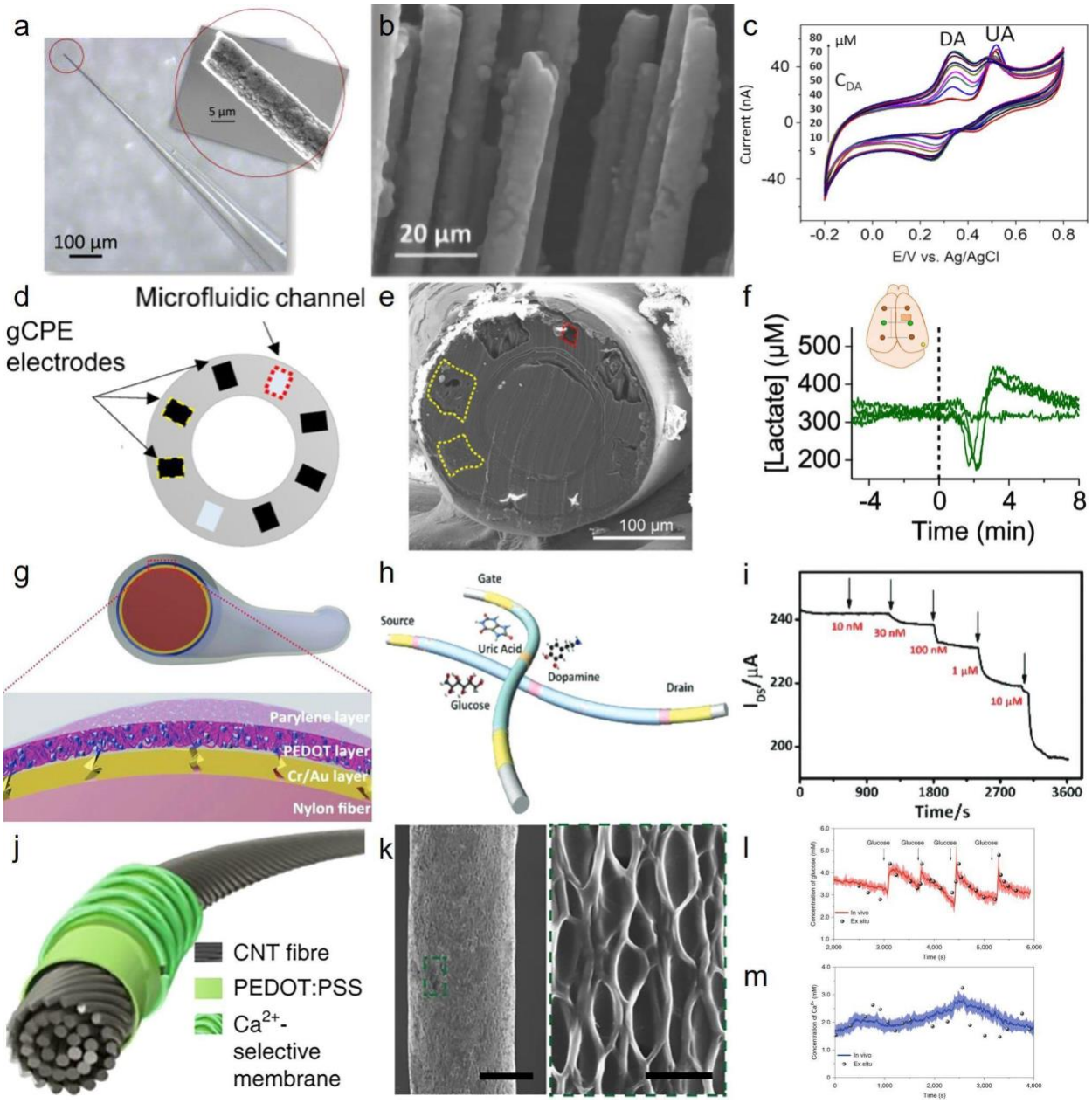

Figure 11 Fibrous implantable sensors. (a) Optical image of diamond coated carbon fiber electrode encapsulated in the glass pipette. The inset shows the SEM image of carbon fiber at the tip of the electrode. (b) SEM image of diamond coated carbon fiber. (c) The cyclic voltammetry

curves obtained in the presence of varying concentrations of dopamine. a–c, Reproduced with permission from Hejazi et al., Biomaterials 230, 119648 (2020). Copyright 2020 Elsevier.[165] (d) The cross-sectional schematics of the fiber made from graphite and conductive polyethylene composite. I SEM cross-section of the fiber with two electrodes highlighted in yellow and a microfluidic channel highlighted in red. (f) Continuous monitoring of lactate in vivo in a mouse model. d–f, Reproduced with permission from Booth et al. Anal. Chem. 93, 6646 (2021); licensed under a Creative Commons Attribution (CC BY) license.[169] (g) Schematics of core-shell structure of conductive nylon fiber with multi-layer coatings. (h) Weaving of fabric organic electrochemical transistors, sensitive to a variety of chemicals. (i) Current response of fabric glucose sensor. g–i, Reproduced with permission from Yang et al., Adv. Mat. 30, 1800051 (2018). Copyright 2018 John Wiley and Sons.[170] (j) Calcium ion sensitive single-ply sensing fibre (SSF) composed of CNT fiber, PEDOT:PSS, and an ion selective membrane. (k) SEM image of SSF and its surface morphology. (l and m), On-body measurement of (l) glucose and Ca^{2+} (m) realized by SSFs and comparison with collected blood samples. Scale bars, 25 μm (left) and 1 μm (right). j–m, reproduced with permission from Wang et al., Nat. Biomed. Eng. 4, 159 (2020). Copyright 2020 Springer Nature.[171]

The detection of chemicals within the body requires a small size of sensors which limits their sensitivity due to decreasing active surface area. While fibers have small sizes, but their surface area is much larger compared to traditional platforms for sensors, exhibiting an excellent option for being an implantable biosensor platform. Apart from monitoring neurotransmitters, fibrous implantable biosensors can be used to monitor important biomarkers within the organs other than the brain. Thanks to the layer-by-layer deposition of functional sensing materials and passivation typically used in chemical sensors, single fibers in the organic electrochemical transistors (OECT) can exhibit sensitivity to a broad range of chemicals (Figure 11g).[170] OECT components can be weaved into each other, realizing sensors for glucose, dopamine, and uric acid (Figure 11h and i).[170] Currently, fibers are now advanced to a new paradigm by further miniaturizing their scales, making it feasible to inject them inside the body (Figure 11j).[171] The CNT single-ply sensing fibers are dip coated inside PEDOT:PSS solution, followed by forming Ca^{2+} membrane cocktail to form a uniform adsorptive layer for sensing calcium ions (Figure 11k).[171] These fibers are injected inside animal models, in this case cat, and measured glucose (Figure 11l) and calcium fluctuations (Figure 11m) in-vivo.[171]

4.6 Implantable fibrous electronics for electrophysiological recording

Electrophysiological recording by fibrous implants is a technique used to measure the electrical activity of cells and tissues in living organisms. It involves the use of fibrous implants, which are thin and flexible electrodes made of conductive materials that can be inserted into biological tissues to record their electrical signals. Fibrous electronic implants offer biocompatibility, porosity for enhanced cell growth, and minimum tissue damage thanks to the geometrical advantages of the fibers. Owing to their low bending stiffness, fibrous platforms are often applied to biological tissues that are most sensitive to external mechanical stimuli such as neurons. The chemo-mechanical mismatch between fibrous implants with neural tissues are often mitigated using materials such as hydrogels and easily integrated to electrical connection to transfer the signals recorded by hydrogel fibers (Figure 12a).[50] The produced fibers are mechanically stable with minimum probe-to-probe variability by maintaining their fibrous structures thanks to an excellent bonding between polymer fibers and hydrogel matrix in hydrated and dehydrated conditions (Figure 12b).[50] These hydrogel-based neural interfaces have similar optically-evoked potential with polymer-based electrodes, while they can still function for over four months inside the human body (Figure 12c).[50] The similar chemo-mechanical properties of hydrogels offer a higher signal to noise ratio and reduced foreign body reaction, exhibited by maintaining the signal quality over a 24 weeks period (Figure 12d).[50] Recording of neural activity is also possible using multi-layered microfibers made from soft CNT core and biocompatible, flexible sodium alginate coating (Figure 12e).[172] These fibers are used as neural implants on the brain (Figure 12f), capable of localized recording of high-fidelity action potentials (Figure 12g).[172] Non-invasive monitoring of deep tissue is not only feasible through fibrous chemical sensors. Fibrous smart sutures made from biocompatible materials such as silk are also capable of monitoring the integrity of tissue, gastric leakage, and tissue micromotion, without a need for indirect observation or costly radiological investigations (Figure 12i).[173] Multiple sensors can be mounted on these sutures (Figure 12j) and wirelessly monitor harmonic backscattering spectra with dynamic dip spectra for leaking detection (Figure 12k).[173]

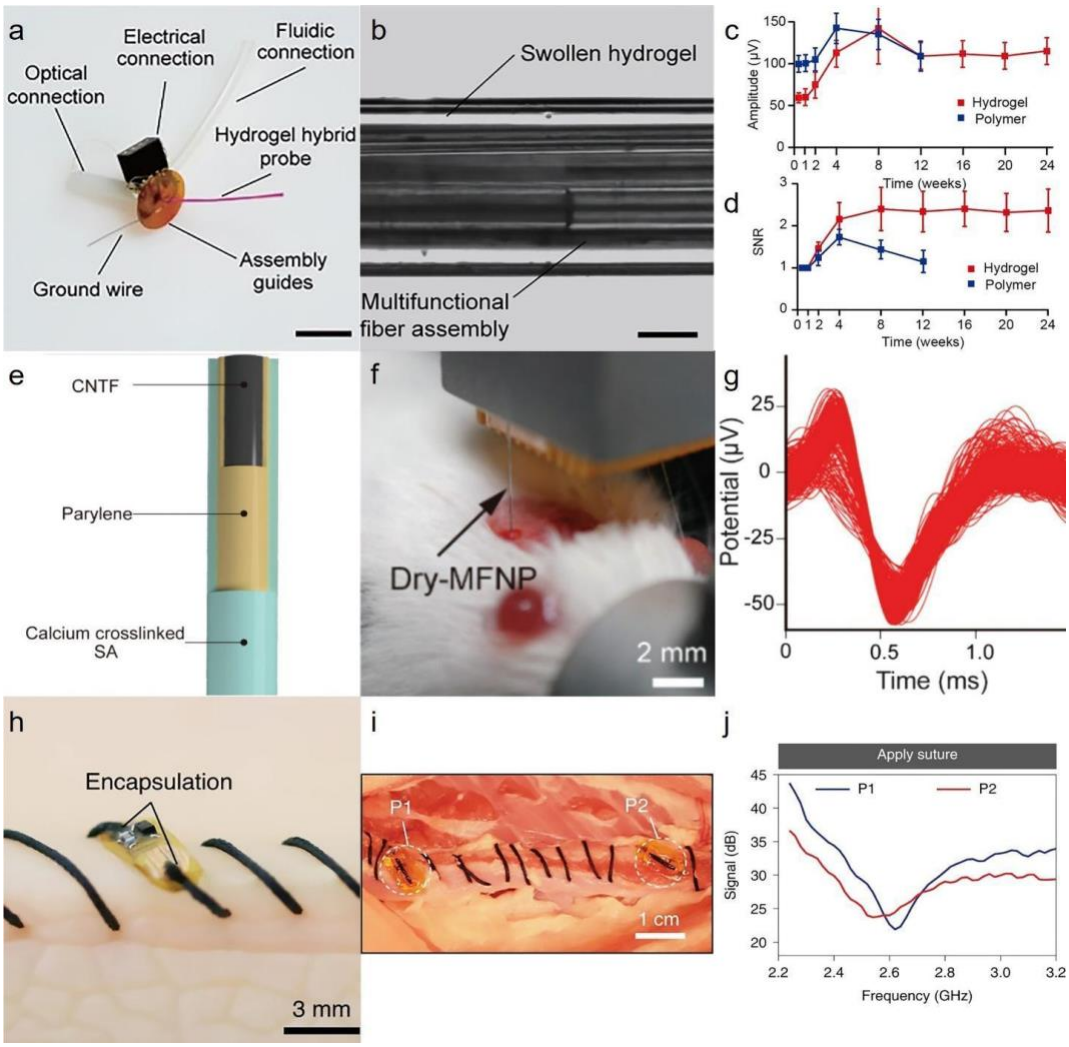

Figure 12 Electrophysiological recording using fibrous bioelectronics. (a) A photograph of neural probe after integration of hydrogel/polymer composite fiber. (b) The microscopic image of the fiber in a swollen state. (c and d) Temporal study of the potential (c) and signal-to-noise ratio (d) recorded by hydrogel hybrid probes and similar polymer probes. a–d, Reproduced with permission from Park et al., Nat. Commun. **12**, 3435 (2021); licensed under a Creative Commons Attribution (CC BY) license.[50] (e) Schematic image of microfiber neural probe made of soft CNT core with sodium alginate shell. (f) Photograph of the fibrous neural probe implanted in a mouse brain. (g) Action potential measurements realized by micro-fibrous neural probe. e–g, Reproduced with permission from Tang et al., J. Mater. Chem. B Mater. Biol. Med. 8, 4387 (2020). Copyright 2020 Royal Society of Chemistry.[172] (h) Snapshot of surgical use for wireless sensing sutures. (i) Integration of multiple sensors for their in-vivo applications. (j) Wireless measurement of harmonic backscattering spectra for application of suture at different frequency range. h–j,

reproduced with permission from Kalidasan et al., Nat. Biomed. Eng. 5, 1217 (2021). Copyright 2021 Springer Nature.[173]

4.7 Implantable fibrous electronics for electrostimulation

Electrostimulation biomedical platforms refer to systems or devices that utilize electrical stimulation to regulate the physiological processes of living organisms, commonly for the purpose of therapy or diagnosis. These platforms can be tailored to stimulate muscles, nerves, or other tissues either locally or across the body and are employed in various clinical settings. Fibers integrated to these systems often work as drug carriers or conductive interfaces mediating tissues with electrical signals produced by biomedical devices. As one of prominent examples, electrospun fibers made from composite materials with magnetic particles and biodegradable polymers are capable of anchoring to the target tissue and maneuvering inside the body using a magnetic field (Figure 13a).[174] Drugs can also be loaded inside these fibers (Figure 13b) and later released in a different physicochemical condition of the surrounding environment (Figure 13c).[174] These fibers can also be stimulated using heat energy and their interaction with thermally sensitive materials. For example, core/shell fibers can release drugs using drug loaded Poly(N-isopropylacrylamide), often known as PNIPAm, mixed with PDMS and Ag concentrated polyurethane (Figure 13d).[175] These fibers are also sutured into porcine skin, and used as tensile sensors for wounds (Figure 13e) while they are controllably releasing the drugs into the target tissue by simply adjusting the number of threads (Figure 13f).[175] Apart from drug delivery purposes, these fibrous platforms are also used for stimulation of tissues by often using electrical or optical signals. Fibers made from natural biocompatible materials such as silk are used to act as optical fibers (Figure 13g) and are easily integrated to electronics for wireless stimulation of neurons (Figure 13h).[176] Mean firing rate of a cortical neuron versus time shows the merit of these fibrous platforms in high-yield, well-isolated, and multi-unit stimulation with a less immunoreactive glial response (Figure 13i,j).[176]

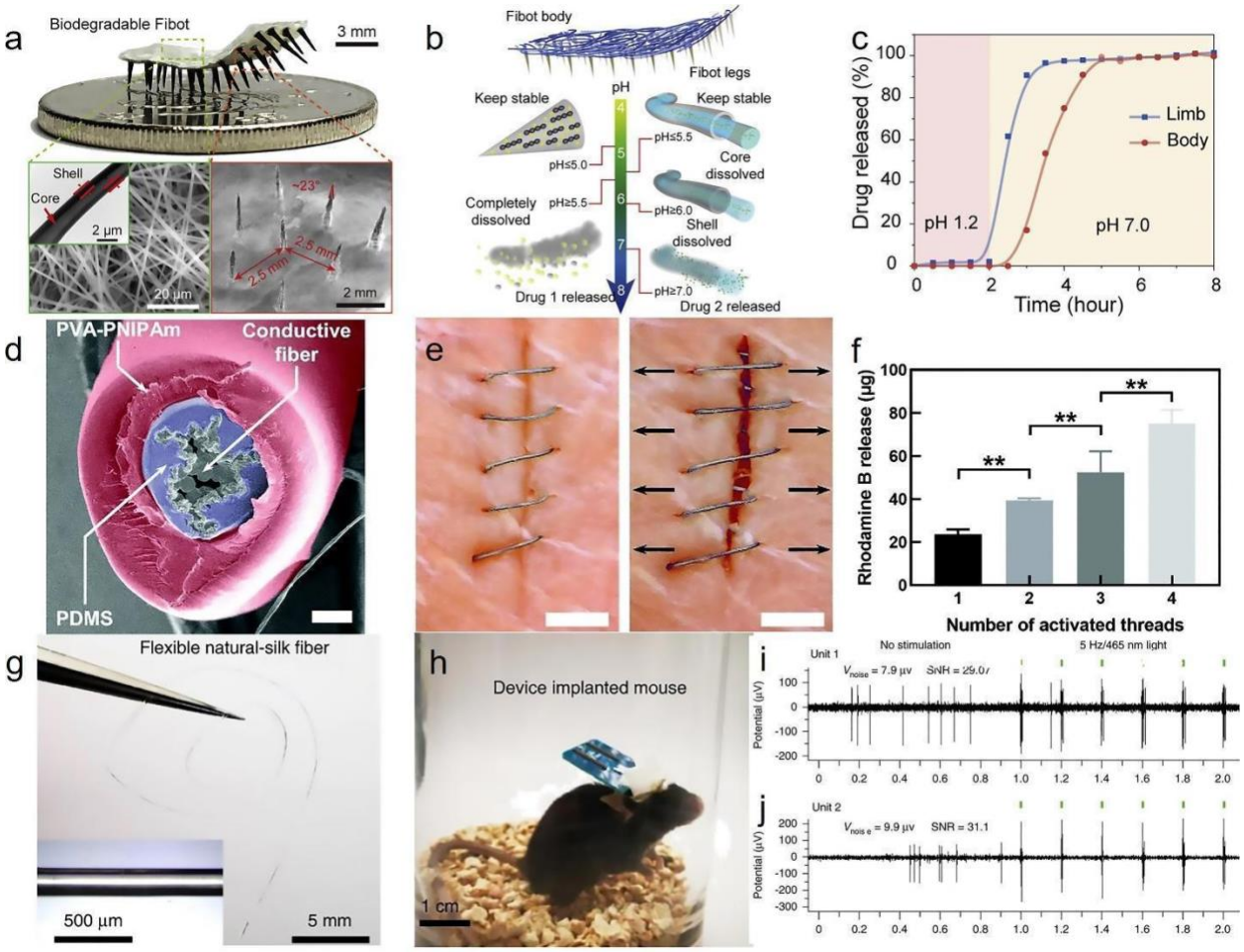

Figure 13 Electrostimulation using fibers. (a) a snapshot of nanofiber-based biodegradable millirobot (Fibot) with SEM (bottom-right) and TEM (bottom-left) images of its core/shell structure. (b and c) pH-responsive drug delivery (b) and its controlled release (c) using Fibot. A–c, Reproduced with permission from Tan et al., Matter 5, 1277 (2022). Copyright 2022 Elsevier.[174] (d) Cross-sectional image of multi-layer fiber, capable of in-situ drug release. (e) Photograph of in-vivo application of fibrous suture. (f) The controlled release of Rhodamine B from the fibrous suture. Scale bar, 100 μm. d–f, Reproduced with permission from Lee et al., Nanoscale 13, 18112 (2021). Copyright 2021 Royal Society of Chemistry.[175] (g) An optical and SEM (inset) image of silk optical fiber. (h) The implantation of the silk optical fiber in a freely moving mouse. Optically evoked action potential for (i) unit 1, and (j) unit 2, exhibiting multi-channel recording capabilities of this fiber-based device. g–j, Reproduced with permission from Zhou et al. Microsyst Nanoeng **8**, 118 (2022); licensed under a Creative Commons Attribution (CC BY) license.[176]

Fibers play a critical role in wearable and implantable devices, typically used in the form of single/few fiber structures or as a durable fibrous network for bioelectronics. In wearable devices, a network of fibers, in the form of either a substrate or a network of fibrous electrodes, is often employed to enable large area sensing and actuation on the skin. On the other hand, in implantable bioelectronics, single fibers are frequently used to minimize invasiveness while maximizing long-term use through the exploitation of the large aspect ratio of fibers.

5. Conclusion and future works

The promise of fibrous structures lies in their potential to provide lightweight, flexible, and biocompatible materials for use in wearable and implantable devices. In this review, we have presented an overview of fiber fabrication techniques, fibrous platforms, and applications of fibers that have propelled research advancements in fibrous wearable and implantable devices. We have highlighted key inventions in manufacturing techniques within three categories: additive manufacturing, spinning, and emerging manufacturing. Additionally, we have summarized research advances in developing platforms for conductive fibers and integrating fibrous interfaces into functioning devices. We have then reviewed the significant progress in developing fibers for wearable and implantable devices in various applications, including thermal management, power generation, sensing, electrostimulation, and electrophysiological recordings. Despite significant breakthroughs in recent decades, the diffusion of most of these biomedical devices remains a major challenge. To address these challenges, we suggest several prospective directions:

(1) Sustainable, large-scale, and low-cost manufacturing of multi-functional fibers. Fibers made from currently available manufacturing methods are compatible with large-scale production, have higher degree of control over fiber morphologies, and are cost-effective. Unfortunately, one single manufacturing platform is not capable of offering all these advantages. The ever-growing quest to find an ideal platform that can make fibers with excellent alignment and controlled morphologies in a large scale with minimum production variability is still an active research area, which can open up the possibilities for larger scale of commercially available fibrous wearables and implants.

(2) Performance stability for the fibers in real-world environments. Current stage of fiber fabrication offers high electrical conductivity, mechanical stability, and excellent sensory performance, capable of real-time measurement of heart, muscle, or brain activity. However,

these produced fibers cannot maintain their excellent conductivity under extreme conditions such as high mechanical strains. Furthermore, application of these fibers on and inside the body is a major challenge over a long period of time as they are not mechanically stable with constant exposure to a variety of mechanical stresses, ranging from small vibrations to major impacts. Moreover, unlike many biological organs such as skin, engineered fibers are not capable of stable sensing performance in a real-world environment with a variety of external stimuli. Although fibers are an ideal geometrical shape for implants due to their flexible and smooth structure, identifying materials for fibers that can effectively mitigate macrophage response remains another significant challenge. Developing fibers with stable electrical, mechanical, or sensory performance from biocompatible materials will be an important step forward to mimic the biological systems or effectively interact with them.

(3) Expansion of sensor functionality for fibrous sensors. Many fibrous sensory platforms for wearable and implantable devices are capable of recording physical and chemical stimuli, ranging from tensile sensors to pulse monitoring with minimal damage to neighboring tissues. While physical fibrous sensors have developed to record stable signals with minimum interferences, chemical sensors capable of quantifying important biomarkers are extremely limited due to the challenges of interferences, extremely low concentrations of important biomarkers, and difficult process of biomarker discovery and its validation.[177] Moreover, in the current stage of their development, fiber sensors are not able to perform selective measurement with no interference from other stimuli in the surrounding environment compared to state-of-the-art sensors,[178] challenging their prolonged use for biomedical purposes. Finding new generations of materials and unique fibrous structures are expected to open up possibilities for realizing chemical and physical sensors with reliable measurements inside the natural environment from our complex human body.

(4) Enhancing the functionality of wearable digital fibers. Fibrous platforms are currently not only connecting electronics thanks to their electroconductive properties but also embed digital devices. However, the nascent field of fibers capable of computing needs to find new ways to store, transfer, or compute information with integrated circuits in a single fiber strand, compatible with large-scale manufacturing. Embedding more complex digital devices in ultrathin fibers promises a future with fibrous textiles that could sense, memorize, learn, and infer from the environments.

Looking forward, the new age of advances in fiber manufacturing and materials promises finding better solutions for some of the most pressing health problems using fibrous wearable and implantable devices. We expect the current review will help in shedding light into major advances in the field of fibrous wearable and implantable devices and display future challenges in the current stage of development for fibrous biomedical devices.

Acknowledgment

This project was supported by the National Institutes of Health grants R01HL155815 and R21DK13266, National Science Foundation grant 2145802, Office of Naval Research grants N00014-21-1-2483 and N00014-21-1-2845, American Cancer Society Research Scholar Grant RSG-21-181-01-CTPS, and Army Research Office grant W911NF-23-1-0041. Behnam Sadri acknowledges the support from National Institutes of Health T32EB023858.

6. References

[1] D.-H. Kim, N. Lu, R. Ma, Y.-S. Kim, R.-H. Kim, S. Wang, J. Wu, S.M. Won, H. Tao, A. Islam, K.J. Yu, T.-I. Kim, R. Chowdhury, M. Ying, L. Xu, M. Li, H.-J. Chung, H. Keum, M. McCormick, P. Liu, Y.-W. Zhang, F.G. Omenetto, Y. Huang, T. Coleman, and J.A. Rogers, Science **333**, 838 (2011).

[2] W. Gao, S. Emaminejad, H.Y.Y. Nyein, S. Challa, K. Chen, A. Peck, H.M. Fahad, H. Ota, H. Shiraki, D. Kiriya, D.-H. Lien, G.A. Brooks, R.W. Davis, and A. Javey, Nature **529**, 509 (2016).

[3] M. Wang, Y. Yang, J. Min, Y. Song, J. Tu, D. Mukasa, C. Ye, C. Xu, N. Heflin, J.S. McCune, T.K. Hsiai, Z. Li, and W. Gao, Nat Biomed Eng **6**, 1225 (2022).

[4] Y. Yang, Y. Song, X. Bo, J. Min, O.S. Pak, L. Zhu, M. Wang, J. Tu, A. Kogan, H. Zhang, T.K. Hsiai, Z. Li, and W. Gao, Nat. Biotechnol. **38**, 217 (2020).

[5] L. Yin and J. Wang, Natl Sci Rev **10**, nwac060 (2023).

[6] H.C. Ates, P.Q. Nguyen, L. Gonzalez-Macia, E. Morales-Narváez, F. Güder, J.J. Collins, and C. Dincer, Nat Rev Mater **7**, 887 (2022).

[7] D.G. Barone, A. Carnicer-Lombarte, P. Tourlomousis, R.S. Hamilton, M. Prater, A.L. Rutz, I.B. Dimov, G.G. Malliaras, S.P. Lacour, A.A.B. Robertson, K. Franze, J.W. Fawcett, and C.E. Bryant, Proc. Natl. Acad. Sci. U. S. A. **119**, e2115857119 (2022).

[8] L. Wang, X. Fu, J. He, X. Shi, T. Chen, P. Chen, B. Wang, and H. Peng, Adv. Mater. **32**, e1901971 (2020).

[9] C. Chen, J. Feng, J. Li, Y. Guo, X. Shi, and H. Peng, Chem. Rev. **123**, 613 (2023).

[10] A. Libanori, G. Chen, X. Zhao, Y. Zhou, and J. Chen, Nature Electronics **5**, 142 (2022).

[11] B.F. Adamu, J. Gao, A.K. Jhatial, and D.M. Kumelachew, Mater. Des. **209**, 109942 (2021).

[12] T. Okoshi, *Optical Fibers* (Elsevier, 2012).

[13] K.C. Kao and G.A. Hockham, Proceedings of the Institution of Electrical Engineers **113**, 1151 (1966).

[14] N.A. Choudhry, L. Arnold, A. Rasheed, I.A. Khan, and L. Wang, Adv. Eng. Mater. **23**, 2100469 (2021).

[15] X. Xu, S. Xie, Y. Zhang, and H. Peng, Angew. Chem. Int. Ed Engl. **58**, 13643 (2019).

[16] J. Wang, T. Ye, Y. Li, L. Wang, L. Li, F. Li, E. He, and Y. Zhang, Polym. J. **54**, 1383 (2022).

[17] Z. Xia, S. Li, G. Wu, Y. Shao, D. Yang, J. Luo, Z. Jiao, J. Sun, and Y. Shao, Adv. Mater. **34**, e2203905 (2022).

[18] S. Ham, M. Kang, S. Jang, J. Jang, S. Choi, T.-W. Kim, and G. Wang, Sci Adv **6**, (2020).

[19] X. Zhang, H. Lin, H. Shang, J. Xu, J. Zhu, and W. Huang, SusMat **1**, 105 (2021).

[20] H. Peng, Adv. Mater. **32**, e1904697 (2020).

[21] G. Loke, W. Yan, T. Khudiyev, G. Noel, and Y. Fink, Adv. Mater. **32**, e1904911 (2020).

[22] W. Zeng, L. Shu, Q. Li, S. Chen, F. Wang, and X.-M. Tao, Adv. Mater. **26**, 5310 (2014).

[23] P. Lu, N. Lalam, M. Badar, B. Liu, B.T. Chorpening, M.P. Buric, and P.R. Ohodnicki, Applied Physics Reviews **6**, 041302 (2019).

[24] P.D. Dragic, M. Cavillon, and J. Ballato, Applied Physics Reviews **5**, 041301 (2018).

[25] K. Peters, Smart Mater. Struct. **20**, 013002 (2010).

[26] P. Gong, X. Li, X. Zhou, Y. Zhang, N. Chen, S. Wang, S. Zhang, and Y. Zhao, Opt. Laser Technol. **139**, 106981 (2021).

[27] Y. Zhao, R.-J. Tong, F. Xia, and Y. Peng, Biosens. Bioelectron. **142**, 111505 (2019).

[28] Z. He and Q. Liu, J. Lightwave Technol. **39**, 3671 (2021).

[29] T. Ma, H.-L. Gao, H.-P. Cong, H.-B. Yao, L. Wu, Z.-Y. Yu, S.-M. Chen, and S.-H. Yu, Adv. Mater. **30**, 1706435 (2018).

[30] D.H. Reneker and I. Chun, Nanotechnology **7**, 216 (1996).

[31] D. Li and Y. Xia, Adv. Mater. **16**, 1151 (2004).

[32] G.I. Taylor and M.D. Van Dyke, Proc. R. Soc. Lond. A Math. Phys. Sci. **313**, 453 (1997).

[33] N. Bhardwaj and S.C. Kundu, Biotechnol. Adv. **28**, 325 (2010).

[34] Y. Li, J. Zhu, H. Cheng, G. Li, H. Cho, M. Jiang, Q. Gao, and X. Zhang, Adv. Mater. Technol. **6**, 2100410 (2021).
[35] J.B. Fenn, M. Mann, C.K. Meng, S.F. Wong, and C.M. Whitehouse, Science **246**, 64 (1989).
[36] Y. Fang, S.L. Zhang, Z.-P. Wu, D. Luan, and X.W. (david) Lou, Science Advances **7**, (2021).
[37] Y. Xu, G. Shi, J. Tang, R. Cheng, X. Shen, Y. Gu, L. Wu, K. Xi, Y. Zhao, W. Cui, and L. Chen, Sci Adv **6**, (2020).
[38] W.E. King and G.L. Bowlin, Polymers **13**, 1097 (2021).
[39] M. Kanik, S. Orguc, G. Varnavides, J. Kim, T. Benavides, D. Gonzalez, T. Akintilo, C.C. Tasan, A.P. Chandrakasan, Y. Fink, and P. Anikeeva, Science **365**, 145 (2019).
[40] C. Dong, A. Leber, D. Yan, H. Banerjee, S. Laperrousaz, T. Das Gupta, S. Shadman, P.M. Reis, and F. Sorin, Sci Adv **8**, eabo0869 (2022).
[41] C. Lu, S. Park, T.J. Richner, A. Derry, I. Brown, C. Hou, S. Rao, J. Kang, C.T. Mortiz, Y. Fink, and P. Anikeeva, Sci Adv **3**, e1600955 (2017).
[42] S. Zeng, S. Pian, M. Su, Z. Wang, M. Wu, X. Liu, M. Chen, Y. Xiang, J. Wu, M. Zhang, Q. Cen, Y. Tang, X. Zhou, Z. Huang, R. Wang, A. Tunuhe, X. Sun, Z. Xia, M. Tian, M. Chen, X. Ma, L. Yang, J. Zhou, H. Zhou, Q. Yang, X. Li, Y. Ma, and G. Tao, Science **373**, 692 (2021).
[43] D. Zhi, Q. Cheng, A.C. Midgley, Q. Zhang, T. Wei, Y. Li, T. Wang, T. Ma, M. Rafique, S. Xia, Y. Cao, Y. Li, J. Li, Y. Che, M. Zhu, K. Wang, and D. Kong, Sci Adv **8**, eabl3888 (2022).
[44] S. Jiang, D.C. Patel, J. Kim, S. Yang, W.A. Mills 3rd, Y. Zhang, K. Wang, Z. Feng, S. Vijayan, W. Cai, A. Wang, Y. Guo, I.F. Kimbrough, H. Sontheimer, and X. Jia, Nat. Commun. **11**, 6115 (2020).
[45] W. Esposito, L. Martin-Monier, P.-L. Piveteau, B. Xu, D. Deng, and F. Sorin, Nat. Commun. **13**, 6154 (2022).
[46] Z. Wang, T. Wu, Z. Wang, T. Zhang, M. Chen, J. Zhang, L. Liu, M. Qi, Q. Zhang, J. Yang, W. Liu, H. Chen, Y. Luo, and L. Wei, Nat. Commun. **11**, 3842 (2020).
[47] M. Chen, Z. Wang, Q. Zhang, Z. Wang, W. Liu, M. Chen, and L. Wei, Nat. Commun. **12**, 1416 (2021).
[48] C. Dong, A. Leber, T. Das Gupta, R. Chandran, M. Volpi, Y. Qu, T. Nguyen-Dang, N. Bartolomei, W. Yan, and F. Sorin, Nat. Commun. **11**, 3537 (2020).
[49] B. Grena, J.-B. Alayrac, E. Levy, A.M. Stolyarov, J.D. Joannopoulos, and Y. Fink, Nat. Commun. **8**, 364 (2017).

[50] S. Park, H. Yuk, R. Zhao, Y.S. Yim, E.W. Woldeghebriel, J. Kang, A. Canales, Y. Fink, G.B. Choi, X. Zhao, and P. Anikeeva, Nat. Commun. **12**, 3435 (2021).

[51] W. Yan, G. Noel, G. Loke, E. Meiklejohn, T. Khudiyev, J. Marion, G. Rui, J. Lin, J. Cherston, A. Sahasrabudhe, J. Wilbert, I. Wicaksono, R.W. Hoyt, A. Missakian, L. Zhu, C. Ma, J. Joannopoulos, and Y. Fink, Nature **603**, 616 (2022).

[52] M. Rein, V.D. Favrod, C. Hou, T. Khudiyev, A. Stolyarov, J. Cox, C.-C. Chung, C. Chhav, M. Ellis, J. Joannopoulos, and Y. Fink, Nature **560**, 214 (2018).

[53] L. Zheng, M. Zhu, B. Wu, Z. Li, S. Sun, and P. Wu, Sci Adv **7**, (2021).

[54] J. Yuan, W. Neri, C. Zakri, P. Merzeau, K. Kratz, A. Lendlein, and P. Poulin, Science **365**, 155 (2019).

[55] Z. Gao, J. Zhu, S. Rajabpour, K. Joshi, M. Kowalik, B. Croom, Y. Schwab, L. Zhang, C. Bumgardner, K.R. Brown, D. Burden, J.W. Klett, A.C.T. van Duin, L.V. Zhigilei, and X. Li, Sci Adv **6**, eaaz4191 (2020).

[56] H. Park, K.H. Lee, Y.B. Kim, S.B. Ambade, S.H. Noh, W. Eom, J.Y. Hwang, W.J. Lee, J. Huang, and T.H. Han, Sci Adv **4**, eaau2104 (2018).

[57] G. Xin, T. Yao, H. Sun, S.M. Scott, D. Shao, G. Wang, and J. Lian, Science **349**, 1083 (2015).

[58] N. Behabtu, C.C. Young, D.E. Tsentalovich, O. Kleinerman, X. Wang, A.W.K. Ma, E.A. Bengio, R.F. ter Waarbeek, J.J. de Jong, R.E. Hoogerwerf, S.B. Fairchild, J.B. Ferguson, B. Maruyama, J. Kono, Y. Talmon, Y. Cohen, M.J. Otto, and M. Pasquali, Science **339**, 182 (2013).

[59] W. Eom, E. Lee, S.H. Lee, T.H. Sung, A.J. Clancy, W.J. Lee, and T.H. Han, Nat. Commun. **12**, 396 (2021).

[60] W. Eom, H. Shin, R.B. Ambade, S.H. Lee, K.H. Lee, D.J. Kang, and T.H. Han, Nat. Commun. **11**, 2825 (2020).

[61] Y. Hou, Z. Sheng, C. Fu, J. Kong, and X. Zhang, Nat. Commun. **13**, 1227 (2022).

[62] Y. Tian, P. Zhu, X. Tang, C. Zhou, J. Wang, T. Kong, M. Xu, and L. Wang, Nat. Commun. **8**, 1080 (2017).

[63] S. Lin, S. Hu, W. Song, M. Gu, J. Liu, J. Song, Z. Liu, Z. Li, K. Huang, Y. Wu, M. Lei, and H. Wu, Npj Flexible Electronics **6**, 1 (2022).

[64] Y.-L. Li, I.A. Kinloch, and A.H. Windle, Science **304**, 276 (2004).

[65] L.M. Ericson, H. Fan, H. Peng, V.A. Davis, W. Zhou, J. Sulpizio, Y. Wang, R. Booker, J. Vavro, C. Guthy, A.N.G. Parra-Vasquez, M.J. Kim, S. Ramesh, R.K. Saini, C. Kittrell, G. Lavin,

H. Schmidt, W.W. Adams, W.E. Billups, M. Pasquali, W.-F. Hwang, R.H. Hauge, J.E. Fischer, and R.E. Smalley, Science **305**, 1447 (2004).

[66] B. Wang, A. Thukral, Z. Xie, L. Liu, X. Zhang, W. Huang, X. Yu, C. Yu, T.J. Marks, and A. Facchetti, Nat. Commun. **11**, 2405 (2020).

[67] C. Jia, L. Li, Y. Liu, B. Fang, H. Ding, J. Song, Y. Liu, K. Xiang, S. Lin, Z. Li, W. Si, B. Li, X. Sheng, D. Wang, X. Wei, and H. Wu, Nat. Commun. **11**, 3732 (2020).

[68] S. Liu, Y. Wang, X. Ming, Z. Xu, Y. Liu, and C. Gao, Nano Lett. **21**, 5116 (2021).

[69] S. Lin, H. Wang, F. Wu, Q. Wang, X. Bai, D. Zu, J. Song, D. Wang, Z. Liu, Z. Li, N. Tao, K. Huang, M. Lei, B. Li, and H. Wu, Npj Flexible Electronics **3**, 1 (2019).

[70] J. Wang, J. Lin, L. Chen, L. Deng, and W. Cui, Adv. Mater. **34**, e2108325 (2022).

[71] A. Mitchell, U. Lafont, M. Hołyńska, and C. Semprimoschnig, Addit. Manuf. **24**, 606 (2018).

[72] I.H. Kim, S. Choi, J. Lee, J. Jung, J. Yeo, J.T. Kim, S. Ryu, S.-K. Ahn, J. Kang, P. Poulin, and S.O. Kim, Nat. Nanotechnol. **17**, 1198 (2022).

[73] J.R. Raney, B.G. Compton, J. Mueller, T.J. Ober, K. Shea, and J.A. Lewis, Proc. Natl. Acad. Sci. U. S. A. **115**, 1198 (2018).

[74] M. Zhang, M. Zhao, M. Jian, C. Wang, A. Yu, Z. Yin, X. Liang, H. Wang, K. Xia, X. Liang, J. Zhai, and Y. Zhang, Matter **1**, 168 (2019).

[75] Y. Sun, Y. You, W. Jiang, B. Wang, Q. Wu, and K. Dai, Science Advances **6**, eaay1422 (2020).

[76] B. Kong, Y. Chen, R. Liu, X. Liu, C. Liu, Z. Shao, L. Xiong, X. Liu, W. Sun, and S. Mi, Nat. Commun. **11**, 1 (2020).

[77] I. Liashenko, J. Rosell-Llompart, and A. Cabot, Nat. Commun. **11**, 753 (2020).

[78] S. Moon, M.S. Jones, E. Seo, J. Lee, L. Lahann, J.H. Jordahl, K.J. Lee, and J. Lahann, Sci Adv **7**, (2021).

[79] P. Mieszczanek, T.M. Robinson, P.D. Dalton, and D.W. Hutmacher, Adv. Mater. **33**, e2100519 (2021).

[80] L. Su, L. Jing, X. Zeng, T. Chen, H. Liu, Y. Kong, X. Wang, X. Yang, C. Fu, J. Sun, and D. Huang, Adv. Mater. **35**, e2207397 (2023).

[81] J.-U. Park, M. Hardy, S.J. Kang, K. Barton, K. Adair, D.K. Mukhopadhyay, C.Y. Lee, M.S. Strano, A.G. Alleyne, J.G. Georgiadis, P.M. Ferreira, and J.A. Rogers, Nat. Mater. **6**, 782 (2007).

[82] W. Wang, K. Ouaras, A.L. Rutz, X. Li, M. Gerigk, T.E. Naegele, G.G. Malliaras, and Y.Y.S.

Huang, Sci Adv **6**, (2020).

[83] X. Bai, S. Lin, H. Wang, Y. Zong, H. Wang, Z. Huang, D. Li, C. Wang, and H. Wu, Npj Flexible Electronics **2**, 1 (2018).

[84] A. Kamada, A. Levin, Z. Toprakcioglu, Y. Shen, V. Lutz-Bueno, K.N. Baumann, P. Mohammadi, M.B. Linder, R. Mezzenga, and T.P.J. Knowles, Small **16**, e1904190 (2020).

[85] H. Chang, Q. Liu, J.F. Zimmerman, K.Y. Lee, Q. Jin, M.M. Peters, M. Rosnach, S. Choi, S.L. Kim, H.A.M. Ardoña, L.A. MacQueen, C.O. Chantre, S.E. Motta, E.M. Cordoves, and K.K. Parker, Science **377**, 180 (2022).

[86] H. Chang, J. Xu, L.A. Macqueen, Z. Aytac, M.M. Peters, J.F. Zimmerman, T. Xu, P. Demokritou, and K.K. Parker, Nature Food **3**, 428 (2022).

[87] Z. Li, Z. Cui, L. Zhao, N. Hussain, Y. Zhao, C. Yang, X. Jiang, L. Li, J. Song, B. Zhang, Z. Cheng, and H. Wu, Sci Adv **8**, eabn3690 (2022).

[88] S. Guan, J. Wang, X. Gu, Y. Zhao, R. Hou, H. Fan, L. Zou, L. Gao, M. Du, C. Li, and Y. Fang, Science Advances **5**, eaav2842 (2019).

[89] Z. Ni, Z. Zhu, Y. Ji, X. He, X. Fu, W. Yang, and Y. Wang, Nano Lett. **22**, 9396 (2022).

[90] M. Javadzadeh, J. Del Barrio, and C. Sánchez-Somolinos, Adv. Mater. e2209244 (2022).

[91] L. Cao, Q. Liu, J. Ren, W. Chen, Y. Pei, D.L. Kaplan, and S. Ling, Adv. Mater. **33**, e2102500 (2021).

[92] G.M. Gonzalez, J. Ward, J. Song, K. Swana, S.A. Fossey, J.L. Palmer, F.W. Zhang, V.M. Lucian, L. Cera, J.F. Zimmerman, F. John Burpo, and K.K. Parker, Matter **3**, 742 (2020).

[93] Y. Cui, H. Gong, Y. Wang, D. Li, and H. Bai, Adv. Mater. **30**, e1706807 (2018).

[94] C. Yang, X. Jiang, X. Gao, H. Wang, L. Li, N. Hussain, J. Xie, Z. Cheng, Z. Li, J. Yan, M. Zhong, L. Zhao, and H. Wu, Nano Lett. **22**, 7212 (2022).

[95] G. Loke, T. Khudiyev, B. Wang, S. Fu, S. Payra, Y. Shaoul, J. Fung, I. Chatziveroglou, P.-W. Chou, I. Chinn, W. Yan, A. Gitelson-Kahn, J. Joannopoulos, and Y. Fink, Nat. Commun. **12**, 3317 (2021).

[96] S. Lee, D. Sasaki, D. Kim, M. Mori, T. Yokota, H. Lee, S. Park, K. Fukuda, M. Sekino, K. Matsuura, T. Shimizu, and T. Someya, Nat. Nanotechnol. **14**, 156 (2019).

[97] T.-W. Shyr, M.-T. Mou, Y.-H. Chen, and J.-L. He, Surf. Coat. Technol. **405**, 126589 (2021).

[98] L. Hu, G. Zheng, J. Yao, N. Liu, B. Weil, M. Eskilsson, E. Karabulut, Z. Ruan, S. Fan, J.T. Bloking, M.D. McGehee, L. Wågberg, and Y. Cui, Energy Environ. Sci. **6**, 513 (2013).

[99] C. Won, U.-J. Jeong, S. Lee, M. Lee, C. Kwon, S. Cho, K. Yoon, S. Lee, D. Chun, I.-J. Cho, and T. Lee, Adv. Funct. Mater. **32**, 2205145 (2022).

[100] C. Kwon, D. Seong, J. Ha, D. Chun, J.-H. Bae, K. Yoon, M. Lee, J. Woo, C. Won, S. Lee, Y. Mei, K.-I. Jang, D. Son, and T. Lee, Adv. Funct. Mater. **30**, 2005447 (2020).

[101] S. He, C. Lu, and S. Zhang, ACS Appl. Mater. Interfaces **3**, 4744 (2011).

[102] Q. Xu, H. Liu, X. Zhong, B. Jiang, and Z. Ma, ACS Appl. Mater. Interfaces **12**, 36609 (2020).

[103] T. Gao, C. Xu, R. Li, R. Zhang, B. Wang, X. Jiang, M. Hu, Y. Bando, D. Kong, P. Dai, and X.-B. Wang, ACS Nano **13**, 11901 (2019).

[104] C.M. Ajmal, S. Bae, and S. Baik, Small **15**, e1803255 (2019).

[105] C. Jia, Y. Liu, L. Li, J. Song, H. Wang, Z. Liu, Z. Li, B. Li, M. Fang, and H. Wu, Nano Lett. **20**, 4993 (2020).

[106] K.A. Kumar, R. Prabu, and R. Arulraj, AIP Conf. Proc. **2413**, 050002 (2022).

[107] J. Zou, F. Ling, X. Shi, K. Xu, H. Wu, P. Chen, B. Zhang, D. Ta, and H. Peng, Small **17**, e2102052 (2021).

[108] B. Reiser, D. Gerstner, L. Gonzalez-Garcia, J.H.M. Maurer, I. Kanelidis, and T. Kraus, ACS Nano **11**, 4934 (2017).

[109] J. Zhang, S. Seyedin, S. Qin, Z. Wang, S. Moradi, F. Yang, P.A. Lynch, W. Yang, J. Liu, X. Wang, and J.M. Razal, Small **15**, e1804732 (2019).

[110] A. Zhao, T. Lin, Y. Xu, W. Zhang, M. Asif, Y. Sun, and F. Xiao, Biosens. Bioelectron. **205**, 114095 (2022).

[111] W. Ma, W. Li, M. Li, Q. Mao, Z. Pan, J. Hu, X. Li, M. Zhu, and Y. Zhang, Adv. Funct. Mater. **31**, 2100195 (2021).

[112] F. Li, H. Zhao, X. Sun, Y. Yue, Z. Wang, and L. Guo, Matter **5**, 4437 (2022).

[113] H. Kim, Y. Jang, D.Y. Lee, J.H. Moon, J.G. Choi, G.M. Spinks, S. Gambhir, D.L. Officer, G.G. Wallace, and S.J. Kim, ACS Appl. Mater. Interfaces **11**, 31162 (2019).

[114] J. Zhang, S. Seyedin, S. Qin, P.A. Lynch, Z. Wang, W. Yang, X. Wang, and J.M. Razal, J. Mater. Chem. A Mater. Energy Sustain. **7**, 6401 (2019).

[115] Y. Gogotsi and B. Anasori, ACS Nano **13**, 8491 (2019).

[116] V. Kedambaimoole, K. Harsh, K. Rajanna, P. Sen, M.M. Nayak, and S. Kumar, Mater. Adv. **3**, 3784 (2022).

[117] K.S. Novoselov, A.K. Geim, S.V. Morozov, D. Jiang, Y. Zhang, S.V. Dubonos, I.V.

Grigorieva, and A.A. Firsov, Science **306**, 666 (2004).

[118] E. Pop, V. Varshney, and A.K. Roy, MRS Bull. **37**, 1273 (2012).

[119] X. Huang, X. Qi, F. Boey, and H. Zhang, Chem. Soc. Rev. **41**, 666 (2012).

[120] S. Stankovich, D.A. Dikin, G.H.B. Dommett, K.M. Kohlhaas, E.J. Zimney, E.A. Stach, R.D. Piner, S.T. Nguyen, and R.S. Ruoff, Nature **442**, 282 (2006).

[121] H. Chen, M.B. Müller, K.J. Gilmore, G.G. Wallace, and D. Li, Adv. Mater. **20**, 3557 (2008).

[122] A.K. Geim and K.S. Novoselov, Nat. Mater. **6**, 183 (2007).

[123] Z. Almansoori, B. Khorshidi, and B. Sadri, Ultrasonics (2018).

[124] B. Sadri, D. Pernitsky, and M. Sadrzadeh, Colloids Surf. A Physicochem. Eng. Asp. (2017).

[125] J.L. Suter and P.V. Coveney, Sci. Rep. **11**, 22460 (2021).

[126] X.-X. Wang, G.-F. Yu, J. Zhang, M. Yu, S. Ramakrishna, and Y.-Z. Long, Prog. Mater Sci. **115**, 100704 (2021).

[127] K. Koziol, J. Vilatela, A. Moisala, M. Motta, P. Cunniff, M. Sennett, and A. Windle, Science **318**, 1892 (2007).

[128] B. Sadri, D. Goswami, M. Sala de Medeiros, A. Pal, B. Castro, S. Kuang, and R.V. Martinez, ACS Appl. Mater. Interfaces **10**, 31061 (2018).

[129] B. Sadri, D. Goswami, and R.V. Martinez, Micromachines **9**, 420 (2018).

[130] B. Sadri, A.M. Abete, and R.V. Martinez, Nanotechnology **30**, 274003 (2019).

[131] Y. Wang, T. Yokota, and T. Someya, NPG Asia Materials **13**, 1 (2021).

[132] S. Lee, S. Franklin, F.A. Hassani, T. Yokota, M.O.G. Nayeem, Y. Wang, R. Leib, G. Cheng, D.W. Franklin, and T. Someya, Science **370**, 966 (2020).

[133] A. Miyamoto, S. Lee, N.F. Cooray, S. Lee, M. Mori, N. Matsuhisa, H. Jin, L. Yoda, T. Yokota, A. Itoh, M. Sekino, H. Kawasaki, T. Ebihara, M. Amagai, and T. Someya, Nat. Nanotechnol. **12**, 907 (2017).

[134] X. Xiao, X. Xiao, Y. Zhou, X. Zhao, G. Chen, Z. Liu, Z. Wang, C. Lu, M. Hu, A. Nashalian, S. Shen, K. Xie, W. Yang, Y. Gong, W. Ding, P. Servati, C. Han, S.X. Dou, W. Li, and J. Chen, Sci Adv **7**, eabl3742 (2021).

[135] Z. Peng, J. Shi, X. Xiao, Y. Hong, X. Li, W. Zhang, Y. Cheng, Z. Wang, W.J. Li, J. Chen, M.K.H. Leung, and Z. Yang, Nat. Commun. **13**, 7835 (2022).

[136] Y. Song, J. Min, Y. Yu, H. Wang, Y. Yang, H. Zhang, and W. Gao, Sci Adv **6**, (2020).

[137] Y. Yu, J. Nassar, C. Xu, J. Min, Y. Yang, A. Dai, R. Doshi, A. Huang, Y. Song, R. Gehlhar,

A.D. Ames, and W. Gao, Sci Robot **5**, (2020).

[138] Z.L. Wang, ACS Nano **7**, 9533 (2013).

[139] X. Lu, H. Qu, and M. Skorobogatiy, ACS Nano **11**, 2103 (2017).

[140] N. Zhang, F. Huang, S. Zhao, X. Lv, Y. Zhou, S. Xiang, S. Xu, Y. Li, G. Chen, C. Tao, Y. Nie, J. Chen, and X. Fan, Matter **2**, 1260 (2020).

[141] H. Sun, W. Tian, F. Cao, J. Xiong, and L. Li, Adv. Mater. **30**, e1706986 (2018).

[142] Y. Cho, S. Pak, Y.-G. Lee, J.S. Hwang, P. Giraud, G.-H. An, and S. Cha, Adv. Funct. Mater. **30**, 1908479 (2020).

[143] M. Liao, C. Wang, Y. Hong, Y. Zhang, X. Cheng, H. Sun, X. Huang, L. Ye, J. Wu, X. Shi, X. Kang, X. Zhou, J. Wang, P. Li, X. Sun, P. Chen, B. Wang, Y. Wang, Y. Xia, Y. Cheng, and H. Peng, Nat. Nanotechnol. **17**, 372 (2022).

[144] H. Xu, Y. Guo, B. Wu, C. Hou, Q. Zhang, Y. Li, and H. Wang, ACS Appl. Mater. Interfaces **12**, 33297 (2020).

[145] H. Yuan, H. Zhang, K. Huang, Y. Cheng, K. Wang, S. Cheng, W. Li, J. Jiang, J. Li, C. Tu, X. Wang, Y. Qi, and Z. Liu, ACS Nano **16**, 2577 (2022).

[146] S.-Y. Cho, H. Yu, J. Choi, H. Kang, S. Park, J.-S. Jang, H.-J. Hong, I.-D. Kim, S.-K. Lee, H.S. Jeong, and H.-T. Jung, ACS Nano **13**, 9332 (2019).

[147] S.-J. Choi, H. Yu, J.-S. Jang, M.-H. Kim, S.-J. Kim, H.S. Jeong, and I.-D. Kim, Small **14**, e1703934 (2018).

[148] Y. Wang, X. Qing, Q. Zhou, Y. Zhang, Q. Liu, K. Liu, W. Wang, M. Li, Z. Lu, Y. Chen, and D. Wang, Biosens. Bioelectron. **95**, 138 (2017).

[149] I. Richard, B. Schyrr, S. Aiassa, S. Carrara, and F. Sorin, ACS Appl. Mater. Interfaces **13**, 43356 (2021).

[150] X. Zhao, Y. Zhou, J. Xu, G. Chen, Y. Fang, T. Tat, X. Xiao, Y. Song, S. Li, and J. Chen, Nat. Commun. **12**, 6755 (2021).

[151] Y. Wang, S. Lee, T. Yokota, H. Wang, Z. Jiang, J. Wang, M. Koizumi, and T. Someya, Sci Adv **6**, eabb7043 (2020).

[152] S. Lee, A. Reuveny, J. Reeder, S. Lee, H. Jin, Q. Liu, T. Yokota, T. Sekitani, T. Isoyama, Y. Abe, Z. Suo, and T. Someya, Nat. Nanotechnol. **11**, 472 (2016).

[153] T. Sekitani, T. Isoyama, Y. Abe, Z. Suo, and T. Someya, Nature (2016).

[154] M. Ganesana, E. Trikantzopoulos, Y. Maniar, S.T. Lee, and B.J. Venton, Biosens.

Bioelectron. **130**, 103 (2019).

[155] C. Lu, U.P. Froriep, R.A. Koppes, A. Canales, V. Caggiano, J. Selvidge, E. Bizzi, and P. Anikeeva, Adv. Funct. Mater. **24**, 6594 (2014).

[156] A. Canales, X. Jia, U.P. Froriep, R.A. Koppes, C.M. Tringides, J. Selvidge, C. Lu, C. Hou, L. Wei, Y. Fink, and P. Anikeeva, Nat. Biotechnol. **33**, 277 (2015).

[157] M.L. Huffman and B.J. Venton, Analyst **134**, 18 (2009).

[158] J.L. Ponchon, R. Cespuglio, F. Gonon, M. Jouvet, and J.F. Pujol, Anal. Chem. **51**, 1483 (1979).

[159] Y. Tian, L. Mao, T. Okajima, and T. Ohsaka, Biosens. Bioelectron. **21**, 557 (2005).

[160] J.J. Mitala and A.C. Michael, Anal. Chim. Acta **556**, 326 (2006).

[161] J. Li, Y. Liu, L. Yuan, B. Zhang, E.S. Bishop, K. Wang, J. Tang, Y.-Q. Zheng, W. Xu, S. Niu, L. Beker, T.L. Li, G. Chen, M. Diyaolu, A.-L. Thomas, V. Mottini, J.B.-H. Tok, J.C.Y. Dunn, B. Cui, S.P. Paşca, Y. Cui, A. Habtezion, X. Chen, and Z. Bao, Nature **606**, 94 (2022).

[162] X. Wu, J. Feng, J. Deng, Z. Cui, L. Wang, S. Xie, C. Chen, C. Tang, Z. Han, H. Yu, X. Sun, and H. Peng, Science China Chemistry **63**, 1281 (2020).

[163] C. Tang, S. Xie, M. Wang, J. Feng, Z. Han, X. Wu, L. Wang, C. Chen, J. Wang, L. Jiang, P. Chen, X. Sun, and H. Peng, J. Mater. Chem. B Mater. Biol. Med. **8**, 4387 (2020).

[164] Y. Li, A.L. Keller, M.T. Cryan, and A.E. Ross, ACS Meas Sci Au **2**, 96 (2022).

[165] M.A. Hejazi, W. Tong, A. Stacey, A. Soto-Breceda, M.R. Ibbotson, M. Yunzab, M.I. Maturana, A. Almasi, Y.J. Jung, S. Sun, H. Meffin, J. Fang, M.E.M. Stamp, K. Ganesan, K. Fox, A. Rifai, A. Nadarajah, S. Falahatdoost, S. Prawer, N.V. Apollo, and D.J. Garrett, Biomaterials **230**, 119648 (2020).

[166] Y. Li and A.E. Ross, Analyst **145**, 805 (2020).

[167] D.P.M. Saraiva, D.V. Braga, B. Bossard, and M. Bertotti, Molecules **28**, 387 (2023).

[168] X.A. Perez and A.M. Andrews, Anal. Chem. **77**, 818 (2005).

[169] M.A. Booth, S.A.N. Gowers, M. Hersey, I.C. Samper, S. Park, P. Anikeeva, P. Hashemi, M.M. Stevens, and M.G. Boutelle, Anal. Chem. **93**, 6646 (2021).

[170] A. Yang, Y. Li, C. Yang, Y. Fu, N. Wang, L. Li, and F. Yan, Advanced Materials **30**, 1800051 (2018).

[171] L. Wang, S. Xie, Z. Wang, F. Liu, Y. Yang, C. Tang, X. Wu, P. Liu, Y. Li, H. Saiyin, S. Zheng, X. Sun, F. Xu, H. Yu, and H. Peng, Nat Biomed Eng **4**, 159 (2020).

[172] C. Tang, S. Xie, M. Wang, J. Feng, Z. Han, X. Wu, L. Wang, C. Chen, J. Wang, L. Jiang, P. Chen, X. Sun, and H. Peng, J. Mater. Chem. B Mater. Biol. Med. **8**, 4387 (2020).
[173] V. Kalidasan, X. Yang, Z. Xiong, R.R. Li, H. Yao, H. Godaba, S. Obuobi, P. Singh, X. Guan, X. Tian, S.A. Kurt, Z. Li, D. Mukherjee, R. Rajarethinam, C.S. Chong, J.-W. Wang, P.L.R. Ee, W. Loke, B.C.K. Tee, J. Ouyang, C.J. Charles, and J.S. Ho, Nat Biomed Eng **5**, 1217 (2021).
[174] R. Tan, X. Yang, H. Lu, L. Yang, T. Zhang, J. Miao, Y. Feng, and Y. Shen, Matter **5**, 1277 (2022).
[175] Y. Lee, H. Kim, Y. Kim, S. Noh, B. Chun, J. Kim, C. Park, M. Choi, K. Park, J. Lee, and J. Seo, Nanoscale **13**, 18112 (2021).
[176] Y. Zhou, C. Gu, J. Liang, B. Zhang, H. Yang, Z. Zhou, M. Li, L. Sun, T.H. Tao, and X. Wei, Microsyst Nanoeng **8**, 118 (2022).
[177] J.R. Sempionatto, J.A. Lasalde-Ramírez, K. Mahato, J. Wang, and W. Gao, Nat Rev Chem **6**, 899 (2022).
[178] J. Min, J. Tu, C. Xu, H. Lukas, S. Shin, Y. Yang, S.A. Solomon, D. Mukasa, and W. Gao, Chem. Rev. (2023).